

Noname manuscript No.
 (will be inserted by the editor)

On the analysis of spectral deferred corrections for differential-algebraic equations of index one

Matthias Bolten[✉] · Lisa Wimmer[✉]

Received: date / Accepted: date

Abstract In this paper, we present a new SDC scheme for solving semi-explicit DAEs with the ability to be parallelized in which only the differential equations are numerically integrated is presented. In Shu et al. (2007) it was shown that SDC for ODEs achieves one order per iteration. We show that this carries over to the new SDC scheme. The method is derived from the approach of spectral deferred corrections and the idea of enforcing the algebraic constraints without numerical integration as in the approach of ε -embedding in Hairer and Wanner (1996). It enforces the algebraic constraints to be satisfied in each iteration and allows an efficient solve of semi-explicit DAEs with high-accuracy. The proposed scheme is compared with other DAE methods. We demonstrate that the proposed SDC scheme is competitive with Runge-Kutta methods for DAEs in terms of accuracy and its parallelized versions are very efficient in comparison to other SDC methods.

Keywords Spectral deferred corrections · Differential-algebraic equations · Stiff problems · Spectral integration

Mathematics Subject Classification (2020) 34A09 · 65F08 · 65L04 · 65L05 · 65L80

1 Introduction

Consider the general differential-algebraic equations formulated as implicit differential equations (IDEs)

$$\mathbf{0} = \mathbf{F}(t, \mathbf{u}(t), \mathbf{u}'(t)). \quad (1)$$

Matthias Bolten · Lisa Wimmer
 Fakultät für Mathematik und Naturwissenschaften, Bergische Universität Wuppertal,
 Gaußstraße 20, 40297 Wuppertal, Germany
 E-mail: bolten@math.uni-wuppertal.de
 E-mail: wimmer@math.uni-wuppertal.de

Such DAEs naturally arise in many fields, e.g. power systems, chemical engineering etc., in order to describe complex models. For example, in power systems, current-voltage relations describe the dynamics of circuit elements and represent differential equations. Kirchhoff's laws must be satisfied in the circuit and are enforced by constraining the differential equations through algebraic equations. Reaction-diffusion problems describe the interplay of reaction and diffusion between concentrations [3], and algebraic equations are used to impose additional conditions, e.g., on the concentrations densities. Scientists are particularly interested in accurate and efficiently computed numerical solutions for such models. However, when solving DAEs, the mixture of numerical differentiation and integration poses a challenge for numerical solvers [2]. Since algebraic equations in semi-explicit DAEs arise as the stiff limit of a corresponding singular perturbation problem, explicit solvers are impractical as stability constraints force prohibitively small time step sizes. Implicit solvers, on the other hand, are effective for DAEs since they provide the desired order of accuracy and allow larger time step sizes due to their generous stability conditions. Stiffly accurate methods are preferred since they do not suffer from order reduction in the algebraic variables. Common stiffly-accurate solvers with high accuracy are Radau IIA methods that belong to the class of *direct solvers* with minimal order reduction. For index-one problems, order $2M - 1$ is achieved for M collocation nodes in differential and algebraic variables. However, for higher-index problems the order in algebraic variables is reduced [12]. Unlike diagonally implicit Runge-Kutta (DIRK) methods, for which full order cannot be expected in all variables even for index-one problems, differential variables retain full order of accuracy [5]. For large systems, a direct solve of the collocation problem becomes computationally inefficient for Radau solvers.

Spectral deferred corrections (SDC) is a high-order iterative method developed by Dutt et al. [9]. It iteratively solves a series of error equations, and the current solution is corrected by adding the approximated error to the actual solution. In each iteration, the solution is computed via forward substitution where the solve of the system at each node has the same effort as computing an Euler step. For linear problems, SDC can be written as a preconditioned Richardson iteration [13]. Each correction improves the order of the numerical solution by one, up to the maximum order of the underlying spectral quadrature rule [24]. In the last twenty-five years, a lot of work has been done on SDC. Splitting variants were developed for general ordinary differential equations (ODEs) [16], for fast- and slow wave problems [19], and general implicit differential equations [6] to improve the computational efficiency. The idea of SDC was expanded to a grid hierarchy, which led to the multilevel SDC. The convergence of the scheme has been examined in [15] and has already been applied to evolution problems [17]. The parallel framework Parallel-Full-Approximation-Scheme-in-Space-and-Time (PFASST) is build on multilevel SDC that enables *parallelization across the steps* [10]. In [21], a numerical strategy for computing coefficients for parallel preconditioners — used to *parallelize SDC across the method* — was introduced, whereas [7] proposes an

analytical approach to obtain such coefficients. In [20], steps towards SDC with adaptive step size were taken to make the scheme as computationally efficient as possible. Recent progress has been made in applying SDC to DAEs; Huang et al. [14] introduced an SDC method for general IDEs (1) that applies the correction procedure within the DAE. The problem is solved for the gradient of the numerical solution, and the numerical solution is then recovered by spectral integration. Another SDC variant suitable for semi-explicit DAEs is also proposed where numerical integration is only restricted to differential variables. This is more efficient because of the missing differential relation of the algebraic variables. In [18], a comprehensive analysis of the different SDC formulations is performed. Another possibility of treating the problem more efficiently is to split the equations into different parts that allows a implicit-explicit treatment [6]. However, applying the implicit-explicit SDC method becomes inefficient for semi-explicit DAEs. Since there is no numerical integration necessary for the constraints, the solver requires higher computational costs than necessary.

In this work, we propose an SDC method suitable for semi-explicit DAEs that is based on the traditional SDC approach. Numerical integration is restricted only to differential equations, and the constraints are enforced to satisfy them in each iteration. The exploitation of the semi-explicit DAE structure makes the solve more efficient. We analyze the proposed method and show that the result in [24] carries over to the DAE case. Numerical experiments confirm the result. We also study the proposed method parallelized across the method. In comparison with existent DAE solvers, we show that the proposed method is competitive with them at least when it is parallelized. In Section 2, the SDC method is derived and explained in more detail. The extension of SDC to DAEs to derive a new scheme for semi-explicit DAEs is done in Section 3. We also prove that the method gains one order per iteration. In order to confirm the results and show the performance of the presented scheme, numerical experiments are done in Section 4. The work concludes with a conclusion.

2 Spectral deferred corrections

The method of spectral deferred corrections was first developed by Dutt et al. [9]. The section is dedicated to the detailed derivation of the method, in which the intention is to provide an understanding of how the scheme is designed. Consider a system of ODEs for $t \in \mathcal{I} := [t_0, t_1]$

$$\mathbf{u}'(t) = \mathbf{f}(\mathbf{u}(t), t), \quad \mathbf{u}(t_0) = \mathbf{u}_0 \quad (2)$$

with initial condition $\mathbf{u}_0 : \mathcal{I} \rightarrow \mathbb{R}^n$, where $\mathbf{u} : \mathcal{I} \rightarrow \mathbb{R}^n$ is the function to be sought, and $\mathbf{f} : \mathbb{R}^n \times \mathcal{I} \rightarrow \mathbb{R}^n$ denotes the right-hand side of the ODE. The interval length of \mathcal{I} denotes the time step size $\Delta t := t_1 - t_0$. Integrating the differential equation in (2) over the interval \mathcal{I} we obtain Picard's integral

formulation given by

$$\mathbf{u}(t) = \mathbf{u}_0 + \int_{t_0}^t \mathbf{f}(\mathbf{u}(s), s) \, ds. \quad (3)$$

Let $t_0 \leq \tau_1 < \dots < \tau_M \leq t_1$ be a set of M collocation nodes with substeps $\Delta\tau_m := \tau_m - \tau_{m-1}$ for $m = 2, \dots, M$, and $\Delta\tau_1 := \tau_1 - t_0$. In the following, Radau IIA nodes with $\tau_1 = t_0$ are used, implying $\Delta\tau_1 = 0$. The integral equation is approximated by a spectral quadrature rule at each node τ_m

$$\mathbf{u}(\tau_m) = \mathbf{u}(t_0) + \sum_{j=1}^M q_{m,j} \mathbf{f}(\mathbf{u}(\tau_j), \tau_j) \quad (4)$$

with quadrature weights

$$q_{m,j} = \int_{t_0}^{\tau_m} \ell_j(s) \, ds \quad (5)$$

ensuring high accuracy. The function $\ell_j(t)$ denotes the j -th Lagrange polynomial

$$\ell_j(t) = \prod_{i=1, i \neq j}^M \frac{t - \tau_i}{\tau_i - \tau_j}. \quad (6)$$

In general, using the spectral quadrature rule with Radau IIA nodes, the integral over the entire interval \mathcal{I} can be computed with error $\mathcal{O}(\Delta t^{2M-1})$. However, the integrals in Picard's formulation are computed with error $\mathcal{O}(\Delta t^{M+1})$ since the integrals are only defined over subintervals $[t_0, \tau_j]$ for $j = 1, \dots, M$.

Equations (4) are equivalent to the stages in a general implicit Runge-Kutta method represented by the Butcher tableau

$$\begin{array}{c|ccc} c_1 & q_{1,1} & \dots & q_{1,M} \\ \vdots & \vdots & & \vdots \\ c_M & q_{M,1} & \dots & q_{M,M} \\ \hline & b_1 & \dots & b_M \end{array}$$

with weights b_j , $j = 1, \dots, M$ and nodes $c_m \in [0, 1]$, $m = 1, \dots, M$ where $\tau_m = t_0 + c_m \Delta t$. Across all collocation nodes the collocation problem is then given by

$$\mathbf{u} = \mathbf{1}_M \otimes \mathbf{u}_0 + \Delta t \mathbf{Q} \otimes \mathbf{I}_n \mathbf{f}(\mathbf{u}) \quad (7)$$

with $\mathbf{1}_M := (1, \dots, 1)^\top \in \mathbb{R}^M$, the vector of the unknown function at collocation nodes $\mathbf{u} := (\mathbf{u}(\tau_1), \dots, \mathbf{u}(\tau_M))^\top \in \mathbb{R}^{Mn}$, and the vector of corresponding right-hand side evaluations $\mathbf{f}(\mathbf{u}) := (\mathbf{f}(\mathbf{u}(\tau_1), \tau_1), \dots, \mathbf{f}(\mathbf{u}(\tau_M), \tau_M))^\top \in \mathbb{R}^{Mn}$. The matrix $\mathbf{Q} = \{q_{m,j}\}_{m,j=1,\dots,M}$ denotes the spectral integration matrix, and \mathbf{I}_n is the identity matrix of size n . If the last collocation node does

not equal the end of the time step, i.e., $\tau_M < t_1$, the solution at the next time t_1 is obtained by performing the collocation update

$$\mathbf{u}(t_1) = \mathbf{u}_0 + \sum_{j=1}^M b_j \mathbf{f}(\mathbf{u}(\tau_j), \tau_j). \quad (8)$$

The implicit system (7) defines a system of Mn equations with Mn unknowns, and therefore the computation of a solution is an expensive task, especially if n is large. This is the case if the right-hand side stems from the spatial discretization of a partial differential equation, or (2) defines a real-world application, for example.

Instead of solving the system directly, the SDC method iteratively solves a series of correction equations and an improved solution for the next iteration is obtained by correcting the solution of the current approximation. The values at collocation nodes are computed by forward substitution, so that the work at each node is similar to that of an Euler step. This is the original idea in the derivation of the method as in [9] that is repeated below.

Assume a provisional solution $\mathbf{u}^0(t)$ that is computed by a low-order time-stepping method. Let $\mathbf{u}^k(t)$ be an approximation to $\mathbf{u}(t)$ for some index $k \geq 0$, and the error to measure the accuracy of the approximation is $\boldsymbol{\delta}^k(t) := \mathbf{u}(t) - \mathbf{u}^k(t)$ with $\mathbf{u}^k(t_0) = \mathbf{u}_0$. The unknown solution is replaced by using the error, and Picard's formulation (3) becomes

$$\mathbf{u}^k(t) + \boldsymbol{\delta}^k(t) = \mathbf{u}_0 + \int_{t_0}^t \mathbf{f}(\mathbf{u}^k(s) + \boldsymbol{\delta}^k(s), s) ds. \quad (9)$$

An equation for the error is received by

$$\boldsymbol{\delta}^k(t) = \int_{t_0}^t \mathbf{f}(\mathbf{u}^k(s) + \boldsymbol{\delta}^k(s), s) - \mathbf{f}(\mathbf{u}^k(s), s) ds + \mathbf{r}^k(t) \quad (10)$$

with residual function

$$\mathbf{r}^k(t) = \mathbf{u}_0 + \int_{t_0}^t \mathbf{f}(\mathbf{u}^k(s), s) ds - \mathbf{u}^k(s) \quad (11)$$

that is used to monitor the convergence during the iteration process. Evaluating the equation (10) at $t = \tau_m$ and $t = t_0$, and taking the difference gives

$$\begin{aligned} & \boldsymbol{\delta}^k(\tau_m) - \boldsymbol{\delta}^k(t_0) \\ &= \int_{t_0}^{\tau_m} \mathbf{f}(\mathbf{u}^k(s) + \boldsymbol{\delta}^k(s), s) - \mathbf{f}(\mathbf{u}^k(s), s) ds + \mathbf{r}^k(\tau_m) - \mathbf{r}^k(t_0). \end{aligned} \quad (12)$$

For the discretization of (12) the difference of the residual functions is the residual at τ_m itself, i.e.,

$$\mathbf{r}^k(\tau_m) - \mathbf{r}^k(t_0) = \mathbf{u}_0 + \int_{t_0}^{\tau_m} \mathbf{f}(\mathbf{u}^k(s), s) ds - \mathbf{u}^k(\tau_m) = \mathbf{r}^k(\tau_m). \quad (13)$$

If the residual $\mathbf{r}^{\tilde{k}}(\tau_m)$ is zero for any index \tilde{k} , the collocation problem is solved. In order to numerically compute the residual, the spectral quadrature rule is used to discretize the integral. Inserting the discretized quantity of (13)

$$\mathbf{u}_0 + \sum_{j=1}^M q_{m,j} \mathbf{f}(\mathbf{u}^k(\tau_j), \tau_j) - \mathbf{u}^k(\tau_m) \quad (14)$$

into (12) the modified equation is

$$\begin{aligned} \mathbf{u}^k(\tau_m) + \boldsymbol{\delta}^k(\tau_m) &= \mathbf{u}_0 + \int_{t_0}^{\tau_m} \mathbf{f}(\mathbf{u}^k(s) + \boldsymbol{\delta}^k(s), s) - \mathbf{f}(\mathbf{u}^k(s), s) \, ds \\ &\quad + \sum_{j=1}^M q_{m,j} \mathbf{f}(\mathbf{u}^k(\tau_j), \tau_j), \end{aligned} \quad (15)$$

where the error $\boldsymbol{\delta}^k(t_0)$ is zero. The integral in (15) is simply discretized using either the left rectangle rule (as implicit Euler steps) by

$$\begin{aligned} &\int_{t_0}^{\tau_m} \mathbf{f}(\mathbf{u}^k(s) + \boldsymbol{\delta}^k(s), s) - \mathbf{f}(\mathbf{u}^k(s), s) \, ds \\ &\approx \sum_{j=1}^m \Delta\tau_j (\mathbf{f}(\mathbf{u}^k(\tau_j) + \boldsymbol{\delta}^k(\tau_j), \tau_j) - \mathbf{f}(\mathbf{u}^k(\tau_j), \tau_j)), \end{aligned} \quad (16)$$

or the right rectangle rule (as explicit Euler steps) by

$$\begin{aligned} &\int_{t_0}^{\tau_m} \mathbf{f}(\mathbf{u}^k(s) + \boldsymbol{\delta}^k(s), s) - \mathbf{f}(\mathbf{u}^k(s), s) \, ds \\ &\approx \sum_{j=1}^{m-1} \Delta\tau_{j+1} (\mathbf{f}(\mathbf{u}^k(\tau_j) + \boldsymbol{\delta}^k(\tau_j), \tau_j) - \mathbf{f}(\mathbf{u}^k(\tau_j), \tau_j)), \end{aligned} \quad (17)$$

where both quadrature rules are first-order. Assume we have discrete approximations $\mathbf{u}_m^k \approx \mathbf{u}^k(\tau_m)$ to the exact values. The solution is corrected by adding the error to the actual approximation, i.e., $\mathbf{u}_m^{k+1} = \mathbf{u}_m^k + \boldsymbol{\delta}^k(\tau_m)$. Collecting the update equation (15) with the implicit Euler as base integration method (16), the implicit SDC scheme suitable for stiff problems reads

$$\mathbf{u}_m^{k+1} = \mathbf{u}_0 + \sum_{j=1}^m \Delta\tau_j (\mathbf{f}(\mathbf{u}_j^{k+1}, \tau_j) - \mathbf{f}(\mathbf{u}_j^k, \tau_j)) + \sum_{j=1}^M q_{m,j} \mathbf{f}(\mathbf{u}_j^k, \tau_j), \quad (18)$$

and the explicit SDC scheme using the explicit Euler as base integrator (17) in (15) is formulated by

$$\mathbf{u}_m^{k+1} = \mathbf{u}_0 + \sum_{j=1}^{m-1} \Delta\tau_{j+1} (\mathbf{f}(\mathbf{u}_j^{k+1}, \tau_j) - \mathbf{f}(\mathbf{u}_j^k, \tau_j)) + \sum_{j=1}^M q_{m,j} \mathbf{f}(\mathbf{u}_j^k, \tau_j), \quad (19)$$

rather suitable for non-stiff problems.

The implicit scheme (18) requires the solution of an implicit system at each collocation node. Since all $m - 1$ values \mathbf{u}_j^{k+1} are already computed, the solution of the system at node τ_m requires the same work as for one implicit Euler step. The same argument carries to the explicit scheme (19): Here, only the evaluation of the right-hand side is required to update the values which is just as cheap as an explicit Euler step.

Both schemes, the implicit SDC method and the explicit SDC method have the general form

$$\mathbf{u}_m^{k+1} = \mathbf{u}_0 + \sum_{j=1}^m \tilde{q}_{m,j} (\mathbf{f}(\mathbf{u}_j^{k+1}, \tau_j) - \mathbf{f}(\mathbf{u}_j^k, \tau_j)) + \sum_{j=1}^M q_{m,j} \mathbf{f}(\mathbf{u}_j^k, \tau_j), \quad (20)$$

where $\tilde{q}_{m,j}$ are the coefficients of a lower triangular matrix \mathbf{Q}_Δ associated with a low-order quadrature rule. In the community it is well-known that the general SDC scheme using

$$\mathbf{Q}_\Delta^{\text{IE}} = \begin{pmatrix} \Delta\tau_1 & 0 & \dots & 0 \\ \Delta\tau_1 & \Delta\tau_2 & \ddots & \vdots \\ \vdots & \vdots & \ddots & 0 \\ \Delta\tau_1 & \Delta\tau_2 & \dots & \Delta\tau_M \end{pmatrix} \quad \text{and} \quad \mathbf{Q}_\Delta^{\text{EE}} = \begin{pmatrix} 0 & \dots & \dots & 0 \\ \Delta\tau_2 & 0 & & \vdots \\ \vdots & \ddots & \ddots & \vdots \\ \Delta\tau_2 & \dots & \Delta\tau_M & 0 \end{pmatrix} \quad (21)$$

refers to the implicit scheme (18), and the explicit scheme (19), respectively.

The traditional SDC method uses a low-order method to compute a provisional solution at each collocation node to obtain provisional values for \mathbf{u}^0 . Instead, an provisional solution is used that is obtained by spreading the initial condition to each collocation node, i.e., $\mathbf{u}^0 := (\mathbf{u}_0, \dots, \mathbf{u}_0)^\top \in \mathbb{R}^{Mn}$.

2.1 SDC as fixed-point method

The collocation problem (7) as a system of equations can be solved by an iterative method. Equivalently, the system has the form

$$\mathbf{C}(\mathbf{u}) = \mathbf{1}_M \otimes \mathbf{u}_0 \quad (22)$$

with

$$\mathbf{C}(\mathbf{u}) := (\mathbf{I}_{Mn} - \Delta t \mathbf{Q} \otimes \mathbf{I}_n \mathbf{f})(\mathbf{u}). \quad (23)$$

If we apply an preconditioned iterative method of the form

$$\mathbf{P}(\mathbf{u}^{k+1}) = \mathbf{P}(\mathbf{u}^k) + (\mathbf{1}_M \otimes \mathbf{u}_0 - \mathbf{C}(\mathbf{u}^k)) \quad (24)$$

with preconditioner

$$\mathbf{P}(\mathbf{u}) := (\mathbf{I}_{Mn} - \Delta t \mathbf{Q}_\Delta \otimes \mathbf{I}_n \mathbf{f})(\mathbf{u}) \quad (25)$$

we obtain the preconditioned Richardson iteration

$$(\mathbf{I}_{Mn} - \Delta t \mathbf{Q}_\Delta \otimes \mathbf{I}_n \mathbf{f})(\mathbf{u}^{k+1}) = \mathbf{1}_M \otimes \mathbf{u}_0 + (\Delta t (\mathbf{Q} - \mathbf{Q}_\Delta) \otimes \mathbf{I}_n \mathbf{f})(\mathbf{u}) \quad (26)$$

that corresponds to the implicit SDC method (18), or the explicit scheme (19) node by node, depending on the choice of \mathbf{Q}_Δ . We denote the iteration matrix

$$(\mathbf{I}_{Mn} - \Delta t \mathbf{Q}_\Delta \otimes \mathbf{I}_n \mathbf{f})^{-1} \Delta t (\mathbf{Q} - \mathbf{Q}_\Delta) \otimes \mathbf{I}_n \mathbf{f}(\mathbf{u}) \quad (27)$$

of (26) by $\mathbf{K}(\mathbf{u})$.

For the numerical experiments we focus on a certain set of \mathbf{Q}_Δ matrices including $\mathbf{Q}_\Delta^{\text{IE}}$ and $\mathbf{Q}_\Delta^{\text{EF}}$. The matrix $\mathbf{Q}_\Delta^{\text{Picard}} = \mathbf{0}$ yields an explicit scheme and equals the Picard iteration known to be suited for non-stiff problems. The following ones either aim to accelerate the convergence in the scheme than representing common quadrature rules, and these ones are quite new. The development of such matrices began with the observation that the original SDC methods (18) and (19) converges slowly. The "LU-trick" [23] eliminates convergence issues and is the matrix of choice for stiff problems. "St. Martin's LU-trick" [23] was presented in 2015 and it was the first alternative for SDC to the traditional SDC methods to significantly improve the convergence rate. The construction of $\mathbf{Q}_\Delta^{\text{LU}}$ is based on minimizing the spectral radius of the stiff limits of the iteration matrix. The matrix is defined by $\mathbf{Q}_\Delta^{\text{LU}} = \mathbf{U}^T$ where \mathbf{U} is computed from the LU decomposition $\mathbf{Q}^T = \mathbf{LU}$.

In 2025, Čaklović et al. [7] present an analytical and generic approach to compute coefficients for the diagonal matrices $\mathbf{Q}_\Delta^{\text{MIN-SR-S}}$ and $\mathbf{Q}_\Delta^{\text{MIN-SR-NS}}$ enabling parallelization across the method for SDC. The approach aims to minimize the spectral radius by computing the coefficients to get a nilpotent iteration matrix.

3 Spectral deferred corrections for differential-algebraic equations

The idea of the SDC method can be extended to the class of DAEs. The KDC method, first proposed in [14], applies SDC to IDEs and the system is numerically solved with a Newton-Krylov method to the gradient of the unknown function. The function is then recovered by spectral quadrature. Consider the semi-explicit DAE for $t \in \mathcal{I}$

$$\mathbf{y}'(t) = \mathbf{f}(\mathbf{y}(t), \mathbf{z}(t), t), \quad \mathbf{0} = \mathbf{g}(\mathbf{y}(t), \mathbf{z}(t), t), \quad (\mathbf{y}(t_0), \mathbf{z}(t_0)) = (\mathbf{y}_0, \mathbf{z}_0) \quad (28)$$

with initial conditions $\mathbf{y}_0 : \mathcal{I} \rightarrow \mathbb{R}^{n_d}$, $\mathbf{z}_0 : \mathcal{I} \rightarrow \mathbb{R}^{n_a}$, where $\mathbf{y} : \mathcal{I} \rightarrow \mathbb{R}^{n_d}$ is the differential variable, and $\mathbf{z} : \mathcal{I} \rightarrow \mathbb{R}^{n_a}$ is the algebraic variable. $\mathbf{f} : \mathbb{R}^{n_d} \times \mathbb{R}^{n_a} \times \mathcal{I} \rightarrow \mathbb{R}^{n_d}$ denotes the right-hand side of the differential equations, and $\mathbf{g} : \mathbb{R}^{n_d} \times \mathbb{R}^{n_a} \times \mathcal{I} \rightarrow \mathbb{R}^{n_a}$ is the right-hand side of the algebraic constraints. We set n_d as the number of differential equations, and differential variables, and n_a as the number of algebraic constraints, and algebraic variables with $n_d + n_a = n$ the size of the entire system (28). Let \mathbf{J}_f be the Jacobian of \mathbf{f} with

$$\mathbf{J}_f = \begin{pmatrix} \frac{\partial \mathbf{f}_1}{\partial y_1} & \dots & \frac{\partial \mathbf{f}_1}{\partial y_n} & \frac{\partial \mathbf{f}_1}{\partial z_1} & \dots & \frac{\partial \mathbf{f}_1}{\partial z_n} \\ \vdots & & \vdots & \vdots & & \vdots \\ \frac{\partial \mathbf{f}_n}{\partial y_1} & \dots & \frac{\partial \mathbf{f}_n}{\partial y_n} & \frac{\partial \mathbf{f}_n}{\partial z_1} & \dots & \frac{\partial \mathbf{f}_n}{\partial z_n} \end{pmatrix} = (\mathbf{J}_f^y \quad \mathbf{J}_f^z), \quad (29)$$

where \mathbf{J}_f^y and \mathbf{J}_f^z are the parts of the Jacobian with respect to \mathbf{y} and \mathbf{z} . $f_i = f_i(\mathbf{y}(t), \mathbf{z}(t), t)$ are the components of the right-hand side \mathbf{f} with $\mathbf{y}(t) = (y_1(t), \dots, y_n(t))$ and $\mathbf{z}(t) = (z_1(t), \dots, z_n(t))$. The Jacobian \mathbf{J}_g of \mathbf{g} and its parts \mathbf{J}_g^y , \mathbf{J}_g^z are defined in the same way.

In the remainder of this work the system (28) is assumed to have index one, i.e., \mathbf{J}_g^z is nonsingular and bounded. If \mathbf{f} and \mathbf{g} are sufficiently smooth, then the algebraic constraints can be solved to \mathbf{z} in terms of a function $\mathbf{G} : \mathbb{R}^{n_d} \times \mathcal{I} \rightarrow \mathbb{R}^{n_a}$ implied by the implicit function theorem via

$$\mathbf{0} = \mathbf{g}(\mathbf{y}(t), \mathbf{z}(t), t) \Leftrightarrow \mathbf{z}(t) = \mathbf{G}(\mathbf{y}(t), t) \quad (30)$$

for fixed time t . Inserting the function \mathbf{G} into the algebraic constraints, differentiating the left-hand side via chain rule and solving to \mathbf{J}_G the Jacobian of \mathbf{G} is

$$\mathbf{J}_G(\mathbf{y}(t), t) = - \left[(\mathbf{J}_g^z)^{-1} \mathbf{J}_g^y \right] (\mathbf{y}, \mathbf{G}(\mathbf{y}(t), t), t). \quad (31)$$

If the arguments of the Jacobian matrices are clear, they will be omitted from now on for better readability.

With the Jacobian characterization at hand, and under the assumptions of the implicit function theorem, the semi-explicit index-one DAE (28) admits a locally unique solution expressed through \mathbf{G} . This representation allows us to reformulate the DAE as an IDE, for which we now introduce the SDC scheme as it has been done in [14]. Consider the general IDE (1). Since a Picard formulation is not available or at least difficult to extract, the function $\mathbf{u}(t)$ is represented via the fundamental theorem of calculus as

$$\mathbf{u}(t) = \mathbf{u}_0 + \int_{t_0}^t \mathbf{U}(s) \, ds,$$

where $\mathbf{U}(t) := \mathbf{u}'(t)$ denotes the derivative of \mathbf{u} . Then, the problem to be intended to solve is

$$\mathbf{0} = \mathbf{F} \left(t, \mathbf{u}_0 + \int_{t_0}^t \mathbf{U}(s) \, ds, \mathbf{U}(t) \right),$$

and discretizing it via spectral quadrature results in a fully-integrating SDC method reading

$$\mathbf{0} = \mathbf{F} \left(\tau_m, \mathbf{u}_0 + \sum_{j=1}^M (q_{m,j} - \tilde{q}_{m,j}) \mathbf{U}_j^k + \sum_{j=1}^m \tilde{q}_{m,j} \mathbf{U}_j^{k+1}, \mathbf{U}_m^{k+1} \right) \quad (32)$$

that is named by FI-SDC in this work. The implicit system at each node is solved by a Newton-Krylov method. After each iteration k the numerical solution \mathbf{u}_m^{k+1} is recovered by numerical integration

$$\mathbf{u}_m^{k+1} = \mathbf{u}_0 + \sum_{j=1}^M q_{M,j} \mathbf{U}_j^{k+1}$$

for stiffly accurate methods. For semi-explicit DAEs the authors suggest a semi-integrating SDC variant

$$\begin{aligned}\mathbf{Y}_m^{k+1} &= \mathbf{f} \left(\mathbf{y}_0 + \sum_{j=1}^M (q_{m,j} - \tilde{q}_{m,j}) \mathbf{Y}_j^k + \sum_{j=1}^m \tilde{q}_{m,j} \mathbf{Y}_j^{k+1}, \mathbf{z}_m^{k+1} \right) \\ \mathbf{0} &= \mathbf{g} \left(\mathbf{y}_0 + \sum_{j=1}^M (q_{m,j} - \tilde{q}_{m,j}) \mathbf{Y}_j^k + \sum_{j=1}^m \tilde{q}_{m,j} \mathbf{Y}_j^{k+1}, \mathbf{z}_m^{k+1} \right)\end{aligned}\quad (33)$$

denoted as **SI-SDC** where numerical integration is restricted to differential variables. For more details the interested reader is referred to [14].

In order to derive a SDC method for DAEs we choose a different approach than above: The SDC method (20) is applied to the differential equations with subject to the algebraic constraints. Then, the constrained SDC method named as **SDC-C** reads

$$\begin{aligned}\mathbf{y}_m^{k+1} &= \mathbf{y}_0 + \sum_{j=1}^m \tilde{q}_{m,j} (\mathbf{f}(\mathbf{y}_j^{k+1}, \mathbf{z}_j^{k+1}, \tau_j) - \mathbf{f}(\mathbf{y}_j^k, \mathbf{z}_j^k, \tau_j)) \\ &\quad + \sum_{j=1}^M q_{m,j} \mathbf{f}(\mathbf{y}_j^k, \mathbf{z}_j^k, \tau_j), \\ \mathbf{0} &= \mathbf{g}(\mathbf{y}_m^{k+1}, \mathbf{z}_m^{k+1}, \tau_m)\end{aligned}\quad (34)$$

with approximations $\mathbf{y}_m^k \approx \mathbf{y}(\tau_m)$ and $\mathbf{z}_m^k \approx \mathbf{z}(\tau_m)$. The derivation for the constrained SDC scheme is based on the constrained Picard formulation

$$\mathbf{y}(t) = \mathbf{y}_0 + \int_{t_0}^t \mathbf{f}(\mathbf{y}(s), \mathbf{z}(s), s) \, ds \quad \text{s. t.} \quad \mathbf{0} = \mathbf{g}(\mathbf{y}(t), \mathbf{z}(t), t). \quad (35)$$

Note that in the linear case the identity matrix \mathbf{I}_{Mn} in the iteration matrix \mathbf{K} is replaced by a matrix $\mathbf{I}_{n_d,0}$ whose first n_d diagonal entries are equal to one and the remaining n_a entries are zero.

Remark 1 (Algebraic constraints as stiff limit) Let us study the scalar differential equation

$$\varepsilon z'(t) = z(t), \quad z(t_0) = z_0 \quad (36)$$

for an initial condition $z_0 \in \mathbb{R}$ and a perturbation parameter $0 < \varepsilon \ll 1$ where ε introduces stiffness to the problem. We apply an implicit SDC scheme that reads across all collocation nodes

$$(\varepsilon \mathbf{I}_M - \Delta t \mathbf{Q}_\Delta) \mathbf{z}^{k+1} = \varepsilon \mathbf{1}_M \otimes z_0 + \Delta t (\mathbf{Q} - \mathbf{Q}_\Delta) \mathbf{z}^k$$

with solution

$$\mathbf{z}^{k+1} = (\varepsilon \mathbf{I}_M - \Delta t \mathbf{Q}_\Delta)^{-1} (\varepsilon \mathbf{1}_M \otimes z_0 + \Delta t (\mathbf{Q} - \mathbf{Q}_\Delta) \mathbf{z}^k).$$

Setting $\varepsilon = 0$ in (36) that represents the stiff limit leads to a purely algebraic equation, and the solution of the modified scheme for the algebraic equation is

$$\mathbf{z}^{k+1} = (\mathbf{I}_M - \mathbf{Q}_\Delta^{-1} \mathbf{Q}) \mathbf{z}^k.$$

This highlights two key aspects: First, in a semi-explicit DAE (28) the algebraic constraints correspond to the stiff limit of the problem that necessitates their implicit treatment. The matrix $(\mathbf{I}_M - \mathbf{Q}_\Delta^{-1} \mathbf{Q})$ is well-known in the community as representing the stiff limit of the iteration matrix, and certain choices of \mathbf{Q}_Δ matrices are specifically designed for this case (see the introduction of the matrices at the end of Section 2.1). Second, since the purely algebraic equation does not involve any time derivatives, numerical integration is not required for its discretization. As a result, applying a fully-integrating SDC method to a semi-explicit DAE, i.e., one that includes the numerical integration of the algebraic equations, yields an unnecessarily inefficient and inaccurate approach. Moreover, the algebraic equations are not guaranteed to be satisfied, as the method effectively solves a collocation problem rather than enforcing the constraints directly. This improper treatment may also cause the method to become unstable more quickly. While the severity of these issues is problem-dependent, the numerical integration of the algebraic components is generally not recommended in this context.

For the **FI-SDC** and **SI-SDC** methods introduced above, the following remark shows that the algebraic equations only converges to zero instead of being zero in every iteration.

Remark 2 (Convergence in algebraic constraints) For a scalar problem consider the **SI-SDC** scheme (33) across all collocation nodes

$$\begin{aligned} \mathbf{Y}^{k+1} &= \mathbf{f}(\mathbf{y}_0 + \Delta t(\mathbf{Q} - \mathbf{Q}_\Delta)\mathbf{Y}^k + \Delta t\mathbf{Q}_\Delta\mathbf{Y}^{k+1}, \mathbf{z}^{k+1}, \boldsymbol{\tau}), \\ \mathbf{0} &= \mathbf{g}(\mathbf{y}_0 + \Delta t(\mathbf{Q} - \mathbf{Q}_\Delta)\mathbf{Y}^k + \Delta t\mathbf{Q}_\Delta\mathbf{Y}^{k+1}, \mathbf{z}^{k+1}, \boldsymbol{\tau}) \end{aligned} \quad (37)$$

with the vector of collocation nodes $\boldsymbol{\tau} := (\tau_1, \dots, \tau_M)$. Assume the solution of (37) is converged in iteration \hat{k} , i.e., $\mathbf{Y}^{\hat{k}} \approx \mathbf{Y}^{\hat{k}+1}$. We define the converged solutions by \mathbf{Y} and \mathbf{z} . Then, for the algebraic constraints we have

$$\mathbf{0} = \mathbf{g}(\mathbf{y}_0 + \Delta t(\mathbf{Q} - \mathbf{Q}_\Delta)\mathbf{Y} + \Delta t\mathbf{Q}_\Delta\mathbf{Y}, \mathbf{z}, \boldsymbol{\tau}) = \mathbf{g}(\mathbf{y}_0 + \Delta t\mathbf{Q}\mathbf{Y}, \mathbf{z}, \boldsymbol{\tau}). \quad (38)$$

The solution \mathbf{y} is recovered by numerical integration

$$\mathbf{y} = \mathbf{y}_0 + \Delta t\mathbf{Q}\mathbf{Y}.$$

Using this in (38) we obtain

$$\mathbf{0} = \mathbf{g}(\mathbf{y}_0 + \Delta t\mathbf{Q} \frac{1}{\Delta t} \mathbf{Q}^{-1}(\mathbf{y} - \mathbf{y}_0), \mathbf{z}, \boldsymbol{\tau}) = \mathbf{g}(\mathbf{y}, \mathbf{z}, \boldsymbol{\tau}),$$

and the same holds for the **FI-SDC** scheme. In contrast, the algebraic constraints are satisfied in each iteration for **SDC-C** since the method always enforces $\mathbf{0} = \mathbf{g}(\mathbf{y}^k, \mathbf{z}^k, \boldsymbol{\tau})$ to hold.

In [6] an semi-implicit version for general IDEs is presented. The authors suggested the splitting of the right-hand side of the IDE allowing the implicit-explicit treatment. In contrast to their approach, which applies SDC to the entire IDE - including the algebraic constraints - by splitting the right-hand side into implicit and explicit parts, our proposed SDC-C method restricts the spectral integration to the differential equations only and retains the algebraic constraint as an implicit condition in the system.

3.1 Local truncation error of constrained SDC method

It was shown in [24] that the original SDC method improves the numerical solution in each iteration by one order up to that of the underlying quadrature rule. We modify the proof from [24] to show the same result for the constrained SDC method. The proof is based on induction (and corresponds in principle to the proof structure used in [24, Lemma 2.1]): First, we will show that the provisional solution across all collocation nodes obtained by spreading the initial condition to each node are first-order accurate which corresponds to iteration $k = 0$. Note that this is in contrast to the framework of the original SDC method where a provisional solution is computed by a low-order method. Then it is found that the numerical solutions in \mathbf{y} and \mathbf{z} in τ_1 in the k -th iteration are of order $\mathcal{O}(\Delta t^{k+1})$. This represents the base case for the assumption that solutions on an arbitrary collocation node are of order $\mathcal{O}(\Delta t^{k+1})$ after k iterations. The entire structure of the proof is illustrated in Figure 1.

The proof requires some preliminaries formulated in the following lemmas. The quadrature weights of the spectral quadrature rule and those of the low-order rule scales linearly with the time step size Δt .

Lemma 1 *The coefficients $\tilde{q}_{m,j}$ of the matrices \mathbf{Q}_Δ^{IE} and \mathbf{Q}_Δ^{EE} satisfy*

$$\tilde{q}_{m,j} = \mathcal{O}(\Delta t) \quad (39)$$

for $j, m = 1, \dots, M$.

Proof Consider (21).

Lemma 2 *Assume that the quadrature weights $\hat{q}_{m,j}$ result from spectral quadrature to integrate a function over the interval $[-1, 1]$. Then, the weights $q_{m,j}$ for integration over $[t_0, \tau_m]$ satisfy*

$$q_{m,j} = \mathcal{O}(\Delta t). \quad (40)$$

Proof Note that the $\hat{q}_{m,j}$ are independent from Δt . To integrate a function over $[t_0, \tau_m]$ a change of variables is applied. The transformed quadrature weights are

$$q_{m,j} = \frac{\tau_m - t_0}{2} \hat{q}_{m,j} = \mathcal{O}(\Delta t). \quad (41)$$

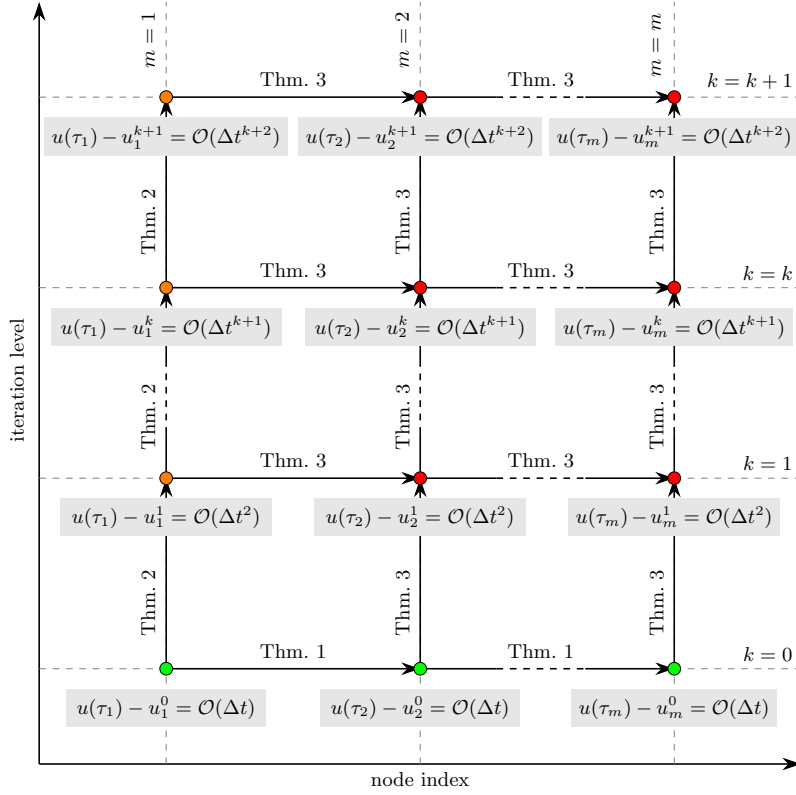


Fig. 1 Structure of induction proof. Green nodes indicate the cases shown by Theorem 1 and present the base case for $k = 0$ and for all m . Orange nodes present cases proven by Theorem 2, they represent the base case for $m = 1$ and all iteration levels k . The red nodes are obtained finally by Theorem 3.

Below the lemmas ensure the boundedness of the Jacobians \mathbf{J}_G , \mathbf{J}_f^y , and \mathbf{J}_f^z , thus the matrices are in $\mathcal{O}(1)$.

Lemma 3 *Let \mathcal{I} be a compact interval. Let \mathbf{y} and \mathbf{z} be continuous functions on that compact interval. Then, the subset*

$$\{t \in \mathcal{I} : (\mathbf{y}(t), \mathbf{z}(t)) \in \mathbb{R}^{n_d} \times \mathbb{R}^{n_a}\} \subset \mathbb{R}^{n_d} \times \mathbb{R}^{n_a}$$

defines a compact subset.

Proof Since \mathbf{y} and \mathbf{z} are continuous on a compact interval, they are bounded by the extreme value theorem.

Lemma 4 *Assume \mathbf{g} is at least a C^1 function, i.e., \mathbf{g} is differentiable and the partial derivatives $\frac{\partial \mathbf{g}_i}{\partial y_j}$ and $\frac{\partial \mathbf{g}_i}{\partial z_j}$ for $i, j = 1, \dots, n$ exist and are continuous. Further, we assume that \mathbf{J}_g^z is invertible. Then, the Jacobian \mathbf{J}_G of function \mathbf{G} in (31) is bounded.*

Proof Applying Lemma 3 the domain of \mathbf{g} denoted as $D := \{(\mathbf{y}(t), \mathbf{z}(t), t) : t \in \mathcal{I}\}$ is a compact subset in $\mathbb{R}^{n_d} \times \mathbb{R}^{n_a} \times \mathcal{I}$. Therefore, the image $\mathbf{g}(D)$ of a continuous function with a compact domain D is compact. Since \mathbf{g} is at least continuously differentiable, the partial derivatives exist and therefore they are bounded.

Differentiating the left-hand side of the equation $\mathbf{g}(\mathbf{y}(t), \mathbf{G}(\mathbf{y}(t), t), t) = \mathbf{0}$ via chain rule and solving to \mathbf{J}_G the Jacobian of \mathbf{G} is given by (31). Due to the invertibility of \mathbf{J}_g^z , both the inverse of \mathbf{J}_g^z and \mathbf{J}_g^y are bounded and thus, \mathbf{J}_G .

Lemma 5 *Assume \mathbf{f} is at least a C^1 function, i.e., \mathbf{f} is differentiable and the partial derivatives $\frac{\partial \mathbf{f}_i}{\partial y_j}$ and $\frac{\partial \mathbf{f}_i}{\partial z_j}$ for $i, j = 1, \dots, n$ exist and are continuous. Then, the Jacobian matrices \mathbf{J}_f^y and \mathbf{J}_f^z are bounded.*

Proof Applying Lemma 3 (as in proof for Lemma 4) already proves what is to be shown.

Define the local errors in \mathbf{y} and \mathbf{z} at node τ_m in iteration k as $\mathbf{e}_{y,m}^k := \mathbf{y}(\tau_m) - \mathbf{y}_m^k$ and $\mathbf{e}_{z,m}^k := \mathbf{z}(\tau_m) - \mathbf{z}_m^k$.

Theorem 1 *Let \mathbf{f} and \mathbf{g} be sufficiently smooth. The problem (28) is assumed to have index one, i.e., the Jacobian part \mathbf{J}_g^z is invertible and it is assumed to be bounded. Then, the provisional solution of the constrained SDC scheme satisfies*

$$\mathbf{e}_{y,m}^0 = \mathcal{O}(\Delta t) \quad \text{and} \quad \mathbf{e}_{z,m}^0 = \mathcal{O}(\Delta t) \quad (42)$$

for $m = 1, \dots, M$.

Proof Subtracting the provisional solution in \mathbf{y} from the evaluated Picard integral equation at $t = \tau_m$ in (35) we have

$$\mathbf{e}_{y,m}^0 = \mathbf{y}(t_0) + \int_{t_0}^{\tau_m} \mathbf{f}(\mathbf{y}(s), \mathbf{z}(s), s) \, ds - \mathbf{y}_0 = \mathcal{O}(\Delta t) \quad (43)$$

by applying the left rectangle rule. Using (30) the local error in \mathbf{z} is

$$\mathbf{e}_{z,m}^0 = \mathbf{G}(\mathbf{y}(\tau_m), \tau_m) - \mathbf{G}(\mathbf{y}_m^0, \tau_m). \quad (44)$$

Expanding $\mathbf{G}(\mathbf{y}_m^0, \tau_m)$ in a Taylor series around $\mathbf{y}(t) = \mathbf{y}(\tau_m)$ by

$$\mathbf{G}(\mathbf{y}_m^0, \tau_m) = \mathbf{G}(\mathbf{y}(\tau_m), \tau_m) - \mathbf{J}_G(\mathbf{y}(\tau_m), \tau_m) \mathbf{e}_{y,m}^0 + \mathcal{O}((\mathbf{e}_{y,m}^0)^2) \quad (45)$$

the error becomes

$$\mathbf{G}(\mathbf{y}(\tau_m), \tau_m) - \mathbf{G}(\mathbf{y}_m^0, \tau_m) = \mathbf{J}_G(\mathbf{y}(\tau_m), \tau_m) \mathbf{e}_{y,m}^0 + \mathcal{O}((\mathbf{e}_{y,m}^0)^2) = \mathcal{O}(\Delta t) \quad (46)$$

due to (43) and Lemma 4.

Remark 3 The original SDC method in [9] uses a provisional solution computed by the implicit Euler, or the explicit Euler that is different to the choice in this work as also noted in Section 2. Nevertheless, spreading the initial condition provides a solution with first-order accuracy as shown above.

Theorem 2 *Under the assumptions of Theorem 1 the numerical solutions in iteration k obtained by the constrained SDC scheme satisfy*

$$\mathbf{e}_{\mathbf{y},1}^k = \mathcal{O}(\Delta t^{k+1}) \quad \text{and} \quad \mathbf{e}_{\mathbf{z},1}^k = \mathcal{O}(\Delta t^{k+1}). \quad (47)$$

Proof (by induction) In the base case the error $\mathbf{e}_{\mathbf{z},1}^1$ at the first node for the constrained scheme can easily be determined by computing the difference

$$\mathbf{e}_{\mathbf{z},1}^1 = \mathbf{G}(\mathbf{y}(\tau_1), \tau_1) - \mathbf{G}(\mathbf{y}_1^1, \tau_1) = \mathbf{J}_{\mathbf{G}}(\mathbf{y}(\tau_1), \tau_1) \mathbf{e}_{\mathbf{y},1}^1 + \mathcal{O}((\mathbf{e}_{\mathbf{y},1}^1)^2), \quad (48)$$

where $\mathbf{G}(\mathbf{y}_1^1, \tau_1)$ is expanded in a Taylor series around $(\mathbf{y}(t), t) = (\mathbf{y}(\tau_1), \tau_1)$

$$\mathbf{G}(\mathbf{y}_1^1, \tau_1) = \mathbf{G}(\mathbf{y}(\tau_1), \tau_1) - \mathbf{J}_{\mathbf{G}}(\mathbf{y}(\tau_1), \tau_1) \mathbf{e}_{\mathbf{y},1}^1 + \mathcal{O}((\mathbf{e}_{\mathbf{y},1}^1)^2)$$

Thus, the local error in \mathbf{z} depends on the local error in \mathbf{y} . For the local error in \mathbf{y} taking the difference of the evaluated Picard integral equation at $t = \tau_1$ in (35) and the first equation in (34) for $k = 1$ leads to

$$\begin{aligned} \mathbf{e}_{\mathbf{y},1}^1 &= \int_{t_0}^{\tau_1} \mathbf{f}(\mathbf{y}(s), \mathbf{z}(s), s) \, ds - \sum_{j=1}^M q_{1,j} \mathbf{f}(\mathbf{y}_j^0, \mathbf{z}_j^0, \tau_j) \\ &\quad - \tilde{q}_{1,1}(\mathbf{f}(\mathbf{y}_1^1, \mathbf{z}_1^1, \tau_1) - \mathbf{f}(\mathbf{y}_1^0, \mathbf{z}_1^0, \tau_1)). \end{aligned} \quad (49)$$

To estimate the error of the first difference in (49) adding a zero term we obtain

$$\begin{aligned} &\int_{t_0}^{\tau_1} \mathbf{f}(\mathbf{y}(s), \mathbf{z}(s), s) \, ds - \sum_{j=1}^M q_{1,j} \mathbf{f}(\mathbf{y}_j^0, \mathbf{z}_j^0, \tau_j) \\ &= \left(\int_{t_0}^{\tau_1} \mathbf{f}(\mathbf{y}(s), \mathbf{z}(s), s) \, ds - \sum_{j=1}^M q_{1,j} \mathbf{f}(\mathbf{y}(\tau_j), \mathbf{z}(\tau_j), \tau_j) \right) \\ &\quad + \left(\sum_{j=1}^M q_{1,j} \mathbf{f}(\mathbf{y}(\tau_j), \mathbf{z}(\tau_j), \tau_j) - \sum_{j=1}^M q_{1,j} \mathbf{f}(\mathbf{y}_j^0, \mathbf{z}_j^0, \tau_j) \right). \end{aligned}$$

Since the quadrature rule with weights $q_{1,j}$ only requires the values of \mathbf{f} evaluated at the collocation nodes, we can interpret \mathbf{f} evaluated at $(\mathbf{y}(\tau_j), \mathbf{z}(\tau_j), \tau_j)$ for $j = 1, \dots, M$ as an interpolating polynomial with error $\mathcal{O}(\Delta t^M)$. Thus, the error of the difference in the first bracket in (50) is

$$\int_{t_0}^{\tau_1} \mathbf{f}(\mathbf{y}(s), \mathbf{z}(s), s) \, ds - \sum_{j=1}^M q_{1,j} \mathbf{f}(\mathbf{y}(\tau_j), \mathbf{z}(\tau_j), \tau_j) = \mathcal{O}(\Delta t^{M+1}).$$

using Lemma 2. For the difference in the second bracket we obtain

$$\sum_{j=1}^M q_{1,j} \mathbf{f}(\mathbf{y}(\tau_j), \mathbf{z}(\tau_j), \tau_j) - \sum_{j=1}^M q_{1,j} \mathbf{f}(\mathbf{y}_j^0, \mathbf{z}_j^0, \tau_j) = \mathcal{O}(\Delta t^2)$$

via the second-order Taylor series expansion

$$\begin{aligned} \mathbf{f}(\mathbf{y}(\tau_j), \mathbf{z}(\tau_j), \tau_j) &= \mathbf{f}(\mathbf{y}_j^0, \mathbf{z}_j^0, \tau_j) + \mathbf{J}_f^y(\mathbf{y}_j^0, \mathbf{z}_j^0, \tau_j) \mathbf{e}_{y,j}^0 + \mathbf{J}_f^z(\mathbf{y}_j^0, \mathbf{z}_j^0, \tau_j) \mathbf{e}_{z,j}^0 \\ &\quad + \mathcal{O}((\mathbf{e}_{y,j}^0)^2 + (\mathbf{e}_{z,j}^0)^2), \end{aligned}$$

Lemma 2, Lemma 5, and Theorem 1 for $j = 1, \dots, M$. We thus get

$$\int_{t_0}^{\tau_1} \mathbf{f}(\mathbf{y}(s), \mathbf{z}(s), s) \, ds - \sum_{j=1}^M q_{1,j} \mathbf{f}(\mathbf{y}_j^0, \mathbf{z}_j^0, \tau_j) = \mathcal{O}(\Delta t^{\min(2, M+1)}). \quad (50)$$

In total we now have

$$\mathbf{e}_{y,1}^1 = \mathcal{O}(\Delta t^{\min(2, M+1)}) - \tilde{q}_{1,1}(\mathbf{f}(\mathbf{y}_1^1, \mathbf{z}_1^1, \tau_1) - \mathbf{f}(\mathbf{y}_1^0, \mathbf{z}_1^0, \tau_1)).$$

Expanding $\mathbf{f}(\mathbf{y}_1^1, \mathbf{z}_1^1, \tau_1)$ in a second-order Taylor series around $\mathbf{f}(\mathbf{y}_1^0, \mathbf{z}_1^0, \tau_1)$ by

$$\begin{aligned} \mathbf{f}(\mathbf{y}_1^1, \mathbf{z}_1^1, \tau_1) &= \mathbf{f}(\mathbf{y}_1^0, \mathbf{z}_1^0, \tau_1) + \mathbf{J}_f^y(\mathbf{y}_1^0, \mathbf{z}_1^0, \tau_1)(\mathbf{y}_1^1 - \mathbf{y}_1^0) \\ &\quad + \mathbf{J}_f^z(\mathbf{y}_1^0, \mathbf{z}_1^0, \tau_1)(\mathbf{z}_1^1 - \mathbf{z}_1^0) + \mathcal{O}((\mathbf{y}_1^1 - \mathbf{y}_1^0)^2 + (\mathbf{z}_1^1 - \mathbf{z}_1^0)^2), \end{aligned}$$

the equation becomes

$$\begin{aligned} \mathbf{e}_{y,1}^1 &= \mathcal{O}(\Delta t^{\min(2, M+1)}) - \tilde{q}_{1,1} \mathbf{J}_f^y(\mathbf{y}_1^0, \mathbf{z}_1^0, \tau_1)(\mathbf{y}_1^1 - \mathbf{y}_1^0) \\ &\quad - \tilde{q}_{1,1} \mathbf{J}_f^z(\mathbf{y}_1^0, \mathbf{z}_1^0, \tau_1)(\mathbf{z}_1^1 - \mathbf{z}_1^0) + \mathcal{O}((\mathbf{y}_1^1 - \mathbf{y}_1^0)^2 + (\mathbf{z}_1^1 - \mathbf{z}_1^0)^2)). \end{aligned} \quad (51)$$

Manipulating the terms $\mathbf{y}_1^1 - \mathbf{y}_1^0$ and $\mathbf{z}_1^1 - \mathbf{z}_1^0$ by adding zeros we obtain for (51)

$$\begin{aligned} \mathbf{e}_{y,1}^1 &= \mathcal{O}(\Delta t^{\min(2, M+1)}) + \tilde{q}_{1,1} \mathbf{J}_f^y(\mathbf{y}_1^0, \mathbf{z}_1^0, \tau_1) \mathbf{e}_{y,1}^1 + \tilde{q}_{1,1} \mathbf{J}_f^z(\mathbf{y}_1^0, \mathbf{z}_1^0, \tau_1) \mathbf{e}_{z,1}^1 \\ &\quad + \mathcal{O}((\mathbf{e}_{y,1}^1)^2 + (\mathbf{e}_{z,1}^1)^2) \end{aligned} \quad (52)$$

via Lemma 1, Lemma 4, Lemma 5, and Theorem 1. Substituting $\mathbf{e}_{z,1}^1$ from (48) to get

$$\begin{aligned} \mathbf{e}_{y,1}^1 &= \mathcal{O}(\Delta t^{\min(2, M+1)}) + \tilde{q}_{1,1} \mathbf{J}_f^y(\mathbf{y}_1^0, \mathbf{z}_1^0, \tau_1) \mathbf{e}_{y,1}^1 \\ &\quad + \tilde{q}_{1,1} \mathbf{J}_f^z(\mathbf{y}_1^0, \mathbf{z}_1^0, \tau_1) \mathbf{J}_G(\mathbf{y}(\tau_1), \tau_1) \mathbf{e}_{y,1}^1 + \mathcal{O}((\mathbf{e}_{y,1}^1)^2 + (\mathbf{e}_{z,1}^1)^2). \end{aligned}$$

Reformulating the equation yields the system

$$\begin{aligned} (\mathbf{I}_{n_d} - \tilde{q}_{1,1} \mathbf{J}_f^y(\mathbf{y}_1^0, \mathbf{z}_1^0, \tau_1) - \tilde{q}_{1,1} \mathbf{J}_f^z(\mathbf{y}_1^0, \mathbf{z}_1^0, \tau_1) \mathbf{J}_G(\mathbf{y}(\tau_1), \tau_1)) \mathbf{e}_{y,1}^1 \\ = \mathcal{O}(\Delta t^{\min(2, M+1)}) + \mathcal{O}((\mathbf{e}_{y,1}^1)^2 + (\mathbf{e}_{z,1}^1)^2). \end{aligned}$$

We assume that the operator on the left-hand side is invertible and the equation can be solved for $e_{\mathbf{y},1}^1$. The Jacobian matrices $\mathbf{J}_f^{\mathbf{y}}$, $\mathbf{J}_f^{\mathbf{z}}$ and \mathbf{J}_G are bounded due to Lemma 4 and Lemma 5 and thus in $\mathcal{O}(1)$. Since the inverse of the left-hand side operator is also in $\mathcal{O}(1)$ we obtain with Lemma 1

$$e_{\mathbf{y},1}^1 = \mathcal{O}(\Delta t^{\min(2,M+1)}), \quad (53)$$

and thus $e_{\mathbf{z},1}^1 = \mathcal{O}(\Delta t^2)$.

We now assume that $e_{\mathbf{y},1}^k = \mathcal{O}(\Delta t^{k+1})$ and $e_{\mathbf{z},1}^k = \mathcal{O}(\Delta t^{k+1})$ for an arbitrary $k < 2M-1$. The local error in \mathbf{z} is expressed by

$$e_{\mathbf{z},1}^{k+1} = \mathbf{G}(\mathbf{y}(\tau_1), \tau_1) - \mathbf{G}(\mathbf{y}_1^{k+1}, \tau_1) = \mathbf{J}_G(\mathbf{y}(\tau_1), \tau_1) e_{\mathbf{y},1}^{k+1} + \mathcal{O}((e_{\mathbf{y},1}^{k+1})^2), \quad (54)$$

again by expanding $\mathbf{G}(\mathbf{y}_1^{k+1}, \tau_1)$ in a Taylor series around $(\mathbf{y}(t), t) = (\mathbf{y}(\tau_1), \tau_1)$ as in (48). Taking the difference of the evaluated Picard integral equation at $t = \tau_1$ in (35) and the $k+1$ -th iterate obtained by the first equation in (34) the local error in \mathbf{y} has the form

$$\begin{aligned} e_{\mathbf{y},1}^{k+1} = & \int_{t_0}^{\tau_1} \mathbf{f}(\mathbf{y}(s), \mathbf{z}(s), s) ds - \sum_{j=1}^M q_{1,j} \mathbf{f}(\mathbf{y}_j^k, \mathbf{z}_j^k, \tau_j) \\ & - \tilde{q}_{1,1}(\mathbf{f}(\mathbf{y}_1^{k+1}, \mathbf{z}_1^{k+1}, \tau_1) - \mathbf{f}(\mathbf{y}_1^k, \mathbf{z}_1^k, \tau_1)). \end{aligned}$$

With the same steps as above and using the induction hypothesis we obtain

$$\int_{t_0}^{\tau_1} \mathbf{f}(\mathbf{y}(s), \mathbf{z}(s), s) ds - \sum_{j=1}^M q_{1,j} \mathbf{f}(\mathbf{y}_j^k, \mathbf{z}_j^k, \tau_j) = \mathcal{O}(\Delta t^{\min(k+2,M+1)})$$

and in total

$$e_{\mathbf{y},1}^{k+1} = \mathcal{O}(\Delta t^{\min(k+2,M+1)}) - \tilde{q}_{1,1}(\mathbf{f}(\mathbf{y}_1^{k+1}, \mathbf{z}_1^{k+1}, \tau_1) - \mathbf{f}(\mathbf{y}_1^k, \mathbf{z}_1^k, \tau_1)).$$

Using a second-order Taylor series expansion as in (51) the error becomes

$$\begin{aligned} e_{\mathbf{y},1}^{k+1} = & \mathcal{O}(\Delta t^{\min(k+2,M+1)}) - \tilde{q}_{1,1} \mathbf{J}_f^{\mathbf{y}}(\mathbf{y}_1^k, \mathbf{z}_1^k, \tau_1)(\mathbf{y}_1^{k+1} - \mathbf{y}_1^k) \\ & - \tilde{q}_{1,1} \mathbf{J}_f^{\mathbf{z}}(\mathbf{y}_1^k, \mathbf{z}_1^k, \tau_1)(\mathbf{z}_1^{k+1} - \mathbf{z}_1^k) + \mathcal{O}((\mathbf{y}_1^{k+1} - \mathbf{y}_1^k)^2 + (\mathbf{z}_1^{k+1} - \mathbf{z}_1^k)^2)). \end{aligned} \quad (55)$$

Adding zero terms in $\mathbf{y}_1^{k+1} - \mathbf{y}_1^k$ and $\mathbf{z}_1^{k+1} - \mathbf{z}_1^k$ and using the induction hypothesis we simply get for (55)

$$\begin{aligned} e_{\mathbf{y},1}^{k+1} = & \mathcal{O}(\Delta t^{\min(k+2,M+1)}) + \tilde{q}_{1,1} \mathbf{J}_f^{\mathbf{y}}(\mathbf{y}_1^k, \mathbf{z}_1^k, \tau_1) e_{\mathbf{y},1}^{k+1} + \tilde{q}_{1,1} \mathbf{J}_f^{\mathbf{z}}(\mathbf{y}_1^k, \mathbf{z}_1^k, \tau_1) e_{\mathbf{z},1}^{k+1} \\ & + \mathcal{O}((e_{\mathbf{y},1}^{k+1})^2 + (e_{\mathbf{z},1}^{k+1})^2) \end{aligned}$$

similar to (52). Substituting $e_{\mathbf{z},1}^{k+1}$ from (54) and reformulating we again receive a system for $e_{\mathbf{y},1}^{k+1}$ given by

$$\begin{aligned} (\mathbf{I}_{n_d} - \tilde{q}_{1,1} \mathbf{J}_f^{\mathbf{y}}(\mathbf{y}_1^k, \mathbf{z}_1^k, \tau_1) - \tilde{q}_{1,1} \mathbf{J}_f^{\mathbf{z}}(\mathbf{y}_1^k, \mathbf{z}_1^k, \tau_1) \mathbf{J}_G(\mathbf{y}(\tau_1), \tau_1)) e_{\mathbf{y},1}^{k+1} \\ = \mathcal{O}(\Delta t^{\min(k+2,M+1)}) + \mathcal{O}((e_{\mathbf{y},1}^{k+1})^2 + (e_{\mathbf{z},1}^{k+1})^2). \end{aligned} \quad (56)$$

We assume that the operator on the left-hand side of the system (56) is invertible. Lemma 4 and Lemma 5 implies the boundedness of \mathbf{J}_f^y , \mathbf{J}_f^z , and \mathbf{J}_G . Thus, they are in $\mathcal{O}(1)$. The inverse of the operator is therefore in $\mathcal{O}(1)$, and we finally obtain with Lemma 1

$$e_{y,1}^{k+1} = \mathcal{O}(\Delta t^{\min(k+2,M+1)}) \quad \text{and} \quad e_{z,1}^{k+1} = \mathcal{O}(\Delta t^{\min(k+2,M+1)}).$$

Theorem 3 *Under the assumptions of Theorem 1 the numerical solutions in iteration k obtained by the constrained SDC scheme satisfy*

$$e_{y,m}^k = \mathcal{O}(\Delta t^{k+1}) \quad \text{and} \quad e_{z,m}^k = \mathcal{O}(\Delta t^{k+1}).$$

for $m = 1, \dots, M$.

Proof (by induction) Theorem 1 and Theorem 2 represent the base case. In the induction hypothesis we assume

$$e_{y,m}^k = \mathcal{O}(\Delta t^{k+1}), \quad e_{z,m}^k = \mathcal{O}(\Delta t^{k+1}) \quad \text{for all } m, \quad (\text{IH1})$$

$$e_{y,\ell}^{k+1} = \mathcal{O}(\Delta t^{k+2}), \quad e_{z,\ell}^{k+1} = \mathcal{O}(\Delta t^{k+2}) \quad \text{with } \ell < m \quad (\text{IH2})$$

for $m = 1, \dots, M$ and $k < 2M - 1$.

We consider the errors in iteration $k + 1$. As in (48) the local error in \mathbf{z} is

$$e_{z,m}^{k+1} = \mathbf{J}_G(\mathbf{y}(\tau_m), \tau_m) e_{y,m}^{k+1} + \mathcal{O}((e_{y,m}^{k+1})^2), \quad (57)$$

via a Taylor series expansion of $\mathbf{G}(\mathbf{y}_m^{k+1}, \tau_m)$ around $(\mathbf{y}(t), t) = (\mathbf{y}(\tau_m), \tau_m)$

$$\mathbf{G}(\mathbf{y}_m^{k+1}, \tau_m) = \mathbf{G}(\mathbf{y}(\tau_m), \tau_m) - \mathbf{J}_G(\mathbf{y}(\tau_m), \tau_m) e_{y,m}^{k+1} + \mathcal{O}((e_{y,m}^{k+1})^2).$$

For the local error in \mathbf{y} we have

$$\begin{aligned} e_{y,m}^{k+1} &= \mathbf{y}(t_0) - \mathbf{y}_0 + \int_{t_0}^{\tau_m} \mathbf{f}(\mathbf{y}(s), \mathbf{z}(s), s) \, ds - \sum_{j=1}^M q_{m,j} \mathbf{f}(\mathbf{y}_j^k, \mathbf{z}_j^k, \tau_j) \\ &\quad - \sum_{j=1}^m \tilde{q}_{m,j} (\mathbf{f}(\mathbf{y}_j^{k+1}, \mathbf{z}_j^{k+1}, \tau_j) - \mathbf{f}(\mathbf{y}_j^k, \mathbf{z}_j^k, \tau_j)). \end{aligned} \quad (58)$$

where the initial conditions $\mathbf{y}(t_0)$ and \mathbf{y}_0 cancel out. The difference representing the interpolation error can be estimated as in the proof for Theorem 2: A zero term is added to the first difference in (58) to yield

$$\begin{aligned} &\int_{t_0}^{\tau_m} \mathbf{f}(\mathbf{y}(s), \mathbf{z}(s), s) \, ds - \sum_{j=1}^M q_{m,j} \mathbf{f}(\mathbf{y}_j^k, \mathbf{z}_j^k, \tau_j) \\ &= \left(\int_{t_0}^{\tau_m} \mathbf{f}(\mathbf{y}(s), \mathbf{z}(s), s) \, ds - \sum_{j=1}^M q_{m,j} \mathbf{f}(\mathbf{y}(\tau_j), \mathbf{z}(\tau_j), \tau_j) \right) \quad (59) \\ &\quad + \left(\sum_{j=1}^M q_{m,j} \mathbf{f}(\mathbf{y}(\tau_j), \mathbf{z}(\tau_j), \tau_j) - \sum_{j=1}^M q_{m,j} \mathbf{f}(\mathbf{y}_j^k, \mathbf{z}_j^k, \tau_j) \right). \end{aligned}$$

The quadrature rule using weights $q_{m,j}$ is interpreted a numerical approximation of the integral of an interpolating polynomial through the points $(\mathbf{y}(\tau_j), \mathbf{z}(\tau_j), \tau_j)$ since the rule only evaluates \mathbf{f} at the collocation nodes τ_j for $j = 1, \dots, M$. The integral is therefore computed with error $\mathcal{O}(\Delta t^M)$, i.e.,

$$\int_{t_0}^{\tau_m} \mathbf{f}(\mathbf{y}(s), \mathbf{z}(s), s) ds - \sum_{j=1}^M q_{m,j} \mathbf{f}(\mathbf{y}(\tau_j), \mathbf{z}(\tau_j), \tau_j) = \mathcal{O}(\Delta t^{M+1}).$$

For the difference in the second bracket we obtain

$$\sum_{j=1}^M q_{m,j} \mathbf{f}(\mathbf{y}(\tau_j), \mathbf{z}(\tau_j), \tau_j) - \sum_{j=1}^M q_{m,j} \mathbf{f}(\mathbf{y}_j^k, \mathbf{z}_j^k, \tau_j) = \mathcal{O}(\Delta t^{k+2})$$

via the second-order Taylor series expansion

$$\begin{aligned} \mathbf{f}(\mathbf{y}(\tau_j), \mathbf{z}(\tau_j), \tau_j) &= \mathbf{f}(\mathbf{y}_j^k, \mathbf{z}_j^k, \tau_j) + \mathbf{J}_f^y(\mathbf{y}_j^k, \mathbf{z}_j^k, \tau_j) \mathbf{e}_{y,j}^k + \mathbf{J}_f^z(\mathbf{y}_j^k, \mathbf{z}_j^k, \tau_j) \mathbf{e}_{z,j}^k \\ &\quad + \mathcal{O}((\mathbf{e}_{y,j}^k)^2 + (\mathbf{e}_{z,j}^k)^2), \end{aligned}$$

Lemma 2, Lemma 4, Lemma 5, and Theorem 1 for $j = 1, \dots, M$. We obtain

$$\int_{t_0}^{\tau_m} \mathbf{f}(\mathbf{y}(s), \mathbf{z}(s), s) ds - \sum_{j=1}^M q_{m,j} \mathbf{f}(\mathbf{y}_j^k, \mathbf{z}_j^k, \tau_j) = \mathcal{O}(\Delta t^{\min(k+2, M+1)}), \quad (60)$$

and in total we have

$$\mathbf{e}_{y,m}^{k+1} = \mathcal{O}(\Delta t^{\min(k+2, M+1)}) - \sum_{j=1}^m \tilde{q}_{m,j} (\mathbf{f}(\mathbf{y}_j^{k+1}, \mathbf{z}_j^{k+1}, \tau_j) - \mathbf{f}(\mathbf{y}_j^k, \mathbf{z}_j^k, \tau_j)).$$

For each $j = 1, \dots, m$ expanding $\mathbf{f}(\mathbf{y}_j^{k+1}, \mathbf{z}_j^{k+1}, \tau_j)$ in a second-order Taylor series around $\mathbf{f}(\mathbf{y}_j^k, \mathbf{z}_j^k, \tau_j)$ by

$$\begin{aligned} \mathbf{f}(\mathbf{y}_j^{k+1}, \mathbf{z}_j^{k+1}, \tau_j) &= \mathbf{f}(\mathbf{y}_j^k, \mathbf{z}_j^k, \tau_j) + \mathbf{J}_f^y(\mathbf{y}_j^k, \mathbf{z}_j^k, \tau_j) (\mathbf{y}_j^{k+1} - \mathbf{y}_j^k) \\ &\quad + \mathbf{J}_f^z(\mathbf{y}_j^k, \mathbf{z}_j^k, \tau_j) (\mathbf{z}_j^{k+1} - \mathbf{z}_j^k) \\ &\quad + \mathcal{O}((\mathbf{y}_j^{k+1} - \mathbf{y}_j^k)^2 + (\mathbf{z}_j^{k+1} - \mathbf{z}_j^k)^2), \end{aligned}$$

the equation becomes

$$\begin{aligned} \mathbf{e}_{y,m}^{k+1} &= \mathcal{O}(\Delta t^{\min(k+2, M+1)}) \\ &\quad - \sum_{j=1}^m \tilde{q}_{m,j} (\mathbf{J}_f^y(\mathbf{y}_j^k, \mathbf{z}_j^k, \tau_j) (\mathbf{y}_j^{k+1} - \mathbf{y}_j^k) + \mathbf{J}_f^z(\mathbf{y}_j^k, \mathbf{z}_j^k, \tau_j) (\mathbf{z}_j^{k+1} - \mathbf{z}_j^k)) \\ &\quad + \mathcal{O}((\mathbf{y}_j^{k+1} - \mathbf{y}_j^k)^2 + (\mathbf{z}_j^{k+1} - \mathbf{z}_j^k)^2)). \end{aligned} \quad (61)$$

Adding zero terms to $\mathbf{y}_j^{k+1} - \mathbf{y}_j^k$ and $\mathbf{z}_j^{k+1} - \mathbf{z}_j^k$ from the induction hypothesis we conclude that

$$\begin{aligned}\mathbf{y}_j^{k+1} - \mathbf{y}_j^k &= \mathbf{y}_j^{k+1} - \mathbf{y}(\tau_j) + \mathbf{y}(\tau_j) - \mathbf{y}_j^k = -\mathbf{e}_{\mathbf{y},j}^{k+1} + \mathcal{O}(\Delta t^{k+1}), \\ \mathbf{z}_j^{k+1} - \mathbf{z}_j^k &= \mathbf{z}_j^{k+1} - \mathbf{z}(\tau_j) + \mathbf{z}(\tau_j) - \mathbf{z}_j^k = -\mathbf{e}_{\mathbf{z},j}^{k+1} + \mathcal{O}(\Delta t^{k+1}).\end{aligned}$$

Therefore, we obtain for (61)

$$\begin{aligned}\mathbf{e}_{\mathbf{y},m}^{k+1} &= \mathcal{O}(\Delta t^{\min(k+2,M+1)}) + \sum_{j=1}^m \tilde{q}_{m,j} (\mathbf{J}_f^{\mathbf{y}}(\mathbf{y}_j^k, \mathbf{z}_j^k, \tau_j) \mathbf{e}_{\mathbf{y},j}^{k+1} + \mathbf{J}_f^{\mathbf{z}}(\mathbf{y}_j^k, \mathbf{z}_j^k, \tau_j) \mathbf{e}_{\mathbf{z},j}^{k+1}) \\ &\quad + \sum_{j=1}^m \mathcal{O}((\mathbf{e}_{\mathbf{y},j}^{k+1})^2 + (\mathbf{e}_{\mathbf{z},j}^{k+1})^2)\end{aligned}$$

via Lemma 1, Lemma 4, Lemma 5, and Theorem 1. Substituting $\mathbf{e}_{\mathbf{z},j}^{k+1}$ from (57) to get

$$\begin{aligned}\mathbf{e}_{\mathbf{y},m}^{k+1} &= \mathcal{O}(\Delta t^{\min(k+2,M+1)}) + \sum_{j=1}^m \tilde{q}_{m,j} \mathbf{J}_f^{\mathbf{y}}(\mathbf{y}_j^k, \mathbf{z}_j^k, \tau_j) \mathbf{e}_{\mathbf{y},j}^{k+1} \\ &\quad + \sum_{j=1}^m \tilde{q}_{m,j} \mathbf{J}_f^{\mathbf{z}}(\mathbf{y}_j^k, \mathbf{z}_j^k, \tau_j) \mathbf{J}_G(\mathbf{y}(\tau_j), \tau_j) \mathbf{e}_{\mathbf{y},j}^{k+1} \\ &\quad + \sum_{j=1}^m \mathcal{O}((\mathbf{e}_{\mathbf{y},j}^{k+1})^2 + (\mathbf{e}_{\mathbf{z},j}^{k+1})^2)\end{aligned}$$

Arranging the first $m-1$ terms of the sum gives

$$\begin{aligned}\mathbf{e}_{\mathbf{y},m}^{k+1} &= \mathcal{O}(\Delta t^{\min(k+2,M+1)}) \\ &\quad + \sum_{j=1}^{m-1} \tilde{q}_{m,j} (\mathbf{J}_f^{\mathbf{y}}(\mathbf{y}_j^k, \mathbf{z}_j^k, \tau_j) + \mathbf{J}_f^{\mathbf{z}}(\mathbf{y}_j^k, \mathbf{z}_j^k, \tau_j) \mathbf{J}_G(\mathbf{y}(\tau_j), \tau_j)) \mathbf{e}_{\mathbf{y},j}^{k+1} \\ &\quad + \tilde{q}_{m,m} (\mathbf{J}_f^{\mathbf{y}}(\mathbf{y}_m^k, \mathbf{z}_m^k, \tau_m) + \mathbf{J}_f^{\mathbf{z}}(\mathbf{y}_m^k, \mathbf{z}_m^k, \tau_m) \mathbf{J}_G(\mathbf{y}(\tau_m), \tau_m)) \mathbf{e}_{\mathbf{y},m}^{k+1} \\ &\quad + \sum_{j=1}^m \mathcal{O}((\mathbf{e}_{\mathbf{y},j}^{k+1})^2 + (\mathbf{e}_{\mathbf{z},j}^{k+1})^2).\end{aligned}$$

From (IH2) it follows that the first $m-1$ summands are even of order $\mathcal{O}(\Delta t^{k+3})$, i.e.,

$$\sum_{j=1}^{m-1} \tilde{q}_{m,j} (\mathbf{J}_f^{\mathbf{y}}(\mathbf{y}_j^k, \mathbf{z}_j^k, \tau_j) + \mathbf{J}_f^{\mathbf{z}}(\mathbf{y}_j^k, \mathbf{z}_j^k, \tau_j) \mathbf{J}_G(\mathbf{y}(\tau_j), \tau_j)) \mathbf{e}_{\mathbf{y},j}^{k+1} = \mathcal{O}(\Delta t^{k+3}),$$

together with Lemma 1, Lemma 4 and Lemma 5. Thus, we obtain

$$\begin{aligned}\mathbf{e}_{\mathbf{y},m}^{k+1} &= \tilde{q}_{m,m} \mathbf{J}_f^{\mathbf{y}}(\mathbf{y}_m^k, \mathbf{z}_m^k, \tau_m) + \tilde{q}_{m,m} \mathbf{J}_f^{\mathbf{z}}(\mathbf{y}_m^k, \mathbf{z}_m^k, \tau_m) \mathbf{J}_G(\mathbf{y}(\tau_m), \tau_m) \mathbf{e}_{\mathbf{y},m}^{k+1} \\ &\quad + \mathcal{O}(\Delta t^{\min(k+2,M+1)}) + \mathcal{O}(((\mathbf{I}_{n_d} + \mathbf{J}_G(\mathbf{y}(\tau_j), \tau_j)) \mathbf{e}_{\mathbf{y},m}^{k+1})^2)\end{aligned}$$

resulting in the system

$$\begin{aligned} (\mathbf{I}_{n_d} - \tilde{q}_{m,m} \mathbf{J}_f^y(\mathbf{y}_m^k, \mathbf{z}_m^k, \tau_m) - \tilde{q}_{m,m} \mathbf{J}_f^z(\mathbf{y}_m^k, \mathbf{z}_m^k, \tau_m) \mathbf{J}_G(\mathbf{y}(\tau_m), \tau_m)) \mathbf{e}_{y,m}^{k+1} \\ = \mathcal{O}(\Delta t^{\min(k+2, M+1)}) + \mathcal{O}(((\mathbf{I}_{n_d} + \mathbf{J}_G(\mathbf{y}(\tau_j), \tau_j)) \mathbf{e}_{y,m}^{k+1})^2). \end{aligned} \quad (62)$$

Lemma 4 and Lemma 5 imply that the Jacobian matrices \mathbf{J}_f^y , \mathbf{J}_f^z and \mathbf{J}_G are bounded. Thus, the inverse of the operator on the left-hand side in (62) is in $\mathcal{O}(1)$ and finally it is

$$\mathbf{e}_{y,m}^{k+1} = \mathcal{O}(\Delta t^{\min(k+2, M+1)}) \quad \text{and} \quad \mathbf{e}_{z,m}^{k+1} = \mathcal{O}(\Delta t^{\min(k+2, M+1)})$$

with Lemma 1.

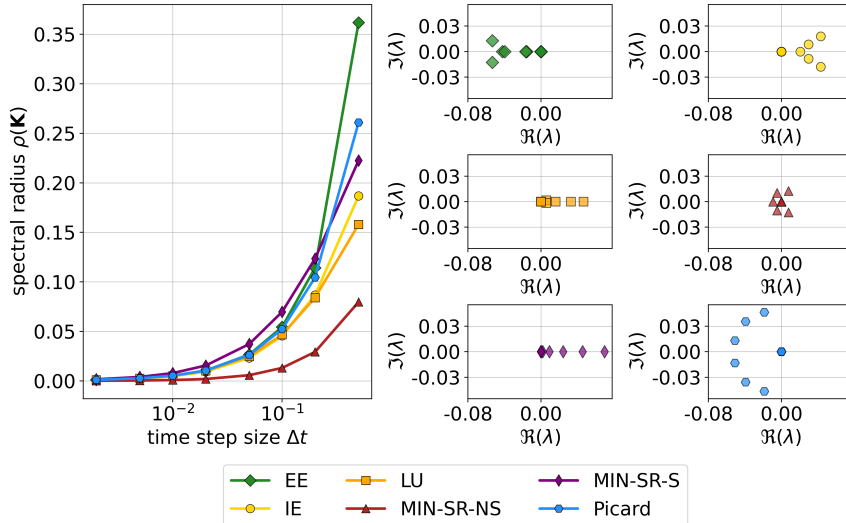


Fig. 2 Spectral radius and eigenvalue distributions of iteration matrix of the constrained SDC scheme for the linear problem (64) for $M = 6$ nodes. Left: Spectral radius for different time step sizes Δt . Right: Eigenvalue distributions (real part versus imaginary part) for $M = 6$ and $\Delta t = 0.01$.

4 Numerical results

In order to evaluate the performance and efficiency of the constrained SDC scheme the numerical experiments are conducted using several choices of the \mathbf{Q}_Δ matrix as introduced in Section 2.1. In particular, we investigate the

scheme using the diagonal matrices $\mathbf{Q}_\Delta^{\text{MIN-SR-NS}}$ and $\mathbf{Q}_\Delta^{\text{MIN-SR-S}}$, which are specifically designed for parallelizing SDC across the method. These simulations are carried out with the Python implementation pySDC [22] using MPI. All SDC variants are used with Radau IIA nodes. The constrained SDC method is evaluated in comparison to the variants FI-SDC and SI-SDC, see Section 3. Instead of using the residual the increment is monitored. We denote the solution to be converged if the increment drops below an error tolerance e_{tol} , i.e.,

$$\|\mathbf{u}^{\tilde{k}+1} - \mathbf{u}^{\tilde{k}}\| < e_{tol}, \quad (63)$$

and \tilde{k} denotes the iteration number at which the solution is converged. For each problem, the error tolerance for each problem is set differently. In general, the tolerance is chosen to be equal to or smaller than 10^{-12} . The vector $u_{M,t}^k$ defines the numerical solution of any unknown \mathbf{u} at some iteration k at the node τ_M at a time t . Note that $\tau_M = t$, the numerical solution is thus the one to the next time step.

The comparison includes Radau IIA methods RadauIIA5 and RadauIIA7 of order 5 and 7, as they are the *methods of choice* when solving DAEs. The class of half-explicit Runge-Kutta methods [11] is quite close to the **SDC-C** method. Thus, we also compare against the Dormand & Prince formula [8] denoted by DOPRI5 being a suitable method in this setting [11]. The computations were carried out on the PLEIADES cluster at the University of Wuppertal. Further details about hardware and software are listed in [4]. The experiments are done for the entire time interval for different time step sizes if not explicitly mentioned.

4.1 Linear problem

First, we study the linear problem

$$\begin{aligned} y'(t) &= -2y(t) + z(t), \\ 0 &= -2y(t) - z(t) \end{aligned} \quad (64)$$

for scalar functions $y(t), z(t) \in \mathbb{R}$. The problem is studied for the time interval $[0, 1]$ with initial conditions $(y_0, z_0) = (1, -2)$, where

$$y(t) = e^{-4t}, \quad z(t) = -2e^{-4t}$$

are exact solutions of the linear problem. The linear implicit system at each node is solved directly.

For the linear problem the **SDC-C** scheme can be written as linear iterative method as described in Section 2.1 allowing a theoretical convergence analysis. The iteration matrix of the **SDC-C** scheme is moderate normal that allows us to study the eigenvalues of it. Figure 2 shows the spectral radius (the largest absolute eigenvalue) and the entire eigenvalue distribution of the iteration matrix of the constrained SDC method for several choices of \mathbf{Q}_Δ across different Δt

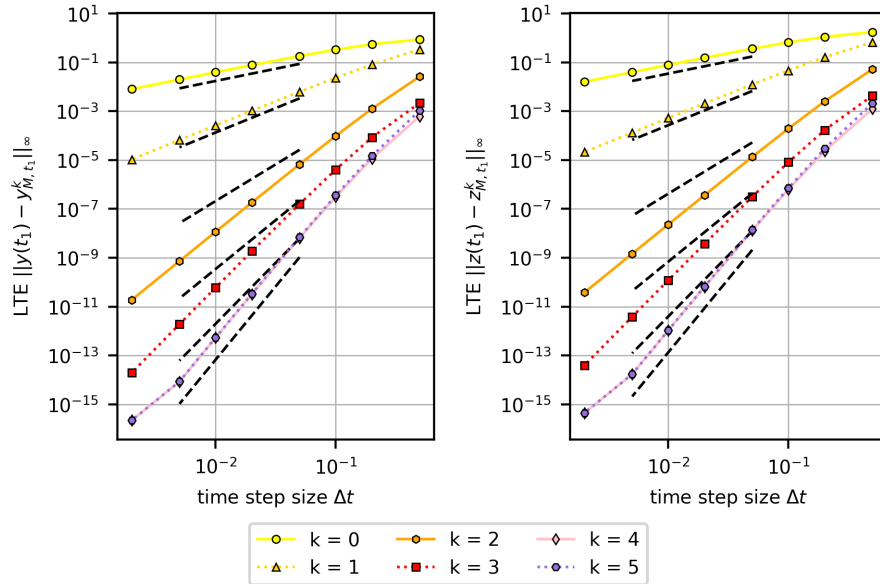


Fig. 3 Local truncation error in y and z against time step sizes Δt for the constrained SDC scheme using $Q_{\Delta}^{\text{MIN-SR-NS}}$ for the linear problem (64) for each iteration $k = 0, \dots, 2M - 1$ with $M = 3$. Black dashed lines indicate the reference order. Left: Error in y . Right: Error in z .

and $M = 6$. The spectral radii only shows the worst case convergence. For instance, the **SDC-C-Picard** scheme exhibits a smaller spectral radius, implying faster convergence for $\Delta t = 0.01$ than the scheme using **MIN-SR-S** preconditioning. Studying the eigenvalue distributions for the **SDC-C-MIN-SR-S** scheme of the right-hand side of the figure we found that there is only one large eigenvalue in magnitude in the distribution and all remaining staying closer to the origin. In contrast, the eigenvalues for the **Picard** iteration form a half circle around the origin with equal distance to it where one of it represents the spectral radius. Numerical experiments confirm that the numerical solution converges faster preconditioned by **MIN-SR-S**.

As mentioned in Remark 2 FI-SDC does lead to errors in the algebraic constraints. Furthermore the non-normality of FI-SDC's iteration matrices renders the approach chosen for analysis here infeasible. Thus, the spectral radii and corresponding eigenvalue distributions do not provide any information about convergence.

The **MIN-SR-NS** preconditioning shows excellent convergence behavior since it has the smallest spectral radius and all its corresponding eigenvalues are clustered around zero. This is expected due to the non-stiff nature of the differential equation.

Figure 3 shows the local truncation error (LTE) for constrained SDC with **MIN-SR-NS** preconditioning in each iteration against time step sizes as predicted by Theorem 3. After $k = 1$ iteration the numerical solutions gain even

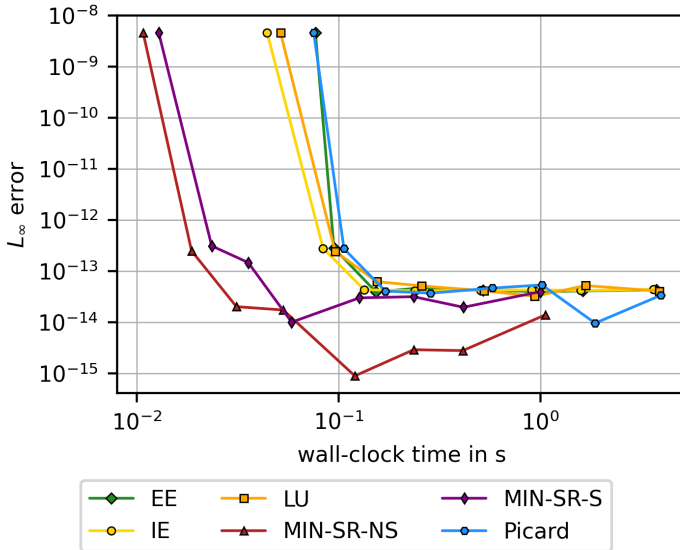


Fig. 4 Wall-clock time against L_∞ error for constrained SDC using $M = 6$ Radau IIA nodes for several choices of Q_Δ across different time step sizes Δt .

two orders such that they achieve a fourth-order accuracy. The maximum order of the underlying quadrature rule is thus already reached after four iterations. The observation was already made in [7] and carries over to the DAE case studied here.

In Figure 4 the costs in terms of wall-clock time against the error of the constrained SDC method for different Q_Δ matrices using $M = 6$ nodes are shown. The parallel schemes are significantly faster than the serial constrained SDC schemes. For larger step sizes MIN-SR-NS preconditioning performs even faster than using the MIN-SR-S preconditioning that is expected since the differential equation is non-stiff and the algebraic constraints representing the stiff limit is treated implicitly but without numerical integration. For large step sizes the scheme with the Picard preconditioner gains a small advantage but in general all sequential schemes have a similar runtime.

The comparison between the SDC variants SDC-C and SI-SDC with LU and MIN-SR-NS preconditioning as well as the comparison with Radau methods and the DOPRI5 method is shown in Figure 5. The parallel SDC variants exhibit a significantly reduced runtime compared to the serial SDC methods. Based on the performance results, SDC-C demonstrates a minor runtime advantage over SI-SDC, suggesting a more cost-efficient formulation. Compared to the tested Runge-Kutta methods, the serial SDC approaches show inferior performance for this particular problem. In contrast, the parallel SDC schemes achieve higher performance than RadauIIA5 and DOPRI5 in terms of runtime. RadauIIA7 remains computationally efficient in this setting, as it computes the solution within each time step by solving a single linear system of dimension

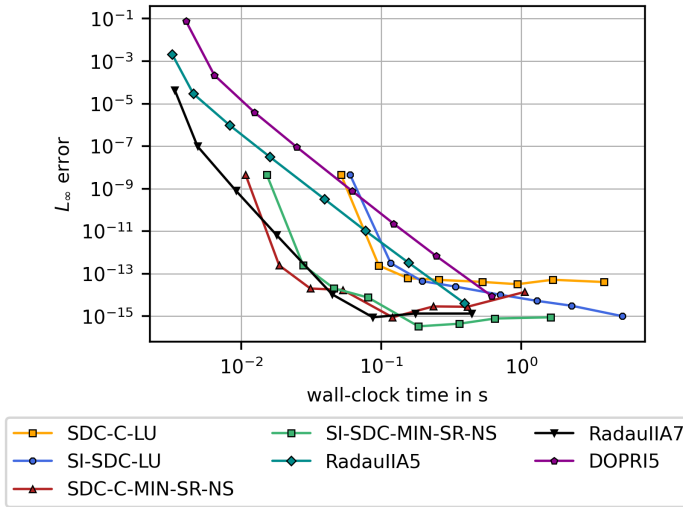


Fig. 5 Wall-clock time versus L_∞ error for different SDC variants using $M = 6$ collocation nodes for LU and MIN-SR-NS preconditioning compared with different Runge-Kutta methods for different time step sizes Δt .

8. In contrast, SDC methods require the solution of multiple linear systems of dimension 2 at every collocation node and during each iteration, which leads to a significantly higher overall runtime. However, the SDC variants offer the advantage of maintaining higher accuracy even for comparatively large time steps, which makes them clearly more favorable than the Runge–Kutta methods with respect to accuracy. For instance, using a time step size of $\Delta t = 0.5$ being the first marker at the plot lines, the numerical solution computed by the SDC methods already achieve an accuracy of less than 10^{-8} where the numerical solution produced by the RadauIIA7 method only reaches an accuracy of less than 10^{-4} .

4.2 Andrews' squeezer

Andrews' squeezing mechanism [1] describes the motions of 7 rigid bodies. The index-1 formulation of the problem is

$$\begin{aligned} \mathbf{q}'(t) &= \mathbf{v}(t), \\ \mathbf{v}'(t) &= \mathbf{w}(t), \\ \mathbf{0} &= \mathbf{M}(\mathbf{q}(t))\mathbf{w}(t) - \mathbf{f}(\mathbf{q}(t), \mathbf{v}(t)) + \mathbf{G}^\top(\mathbf{q}(t))\boldsymbol{\lambda}(t), \\ \mathbf{0} &= \mathbf{g}_{\mathbf{q}\mathbf{q}}(\mathbf{q}(t))(\mathbf{v}(t), \mathbf{v}(t)) + \mathbf{G}(\mathbf{q}(t))\mathbf{w}(t) \end{aligned} \quad (65)$$

with differential variables $\mathbf{q}(t), \mathbf{v}(t) \in \mathbb{R}^7$, and algebraic variables $\mathbf{w}(t) \in \mathbb{R}^7$, $\boldsymbol{\lambda}(t) \in \mathbb{R}^6$ for $0 \leq t \leq 0.03$. The original problem of index three replaces the

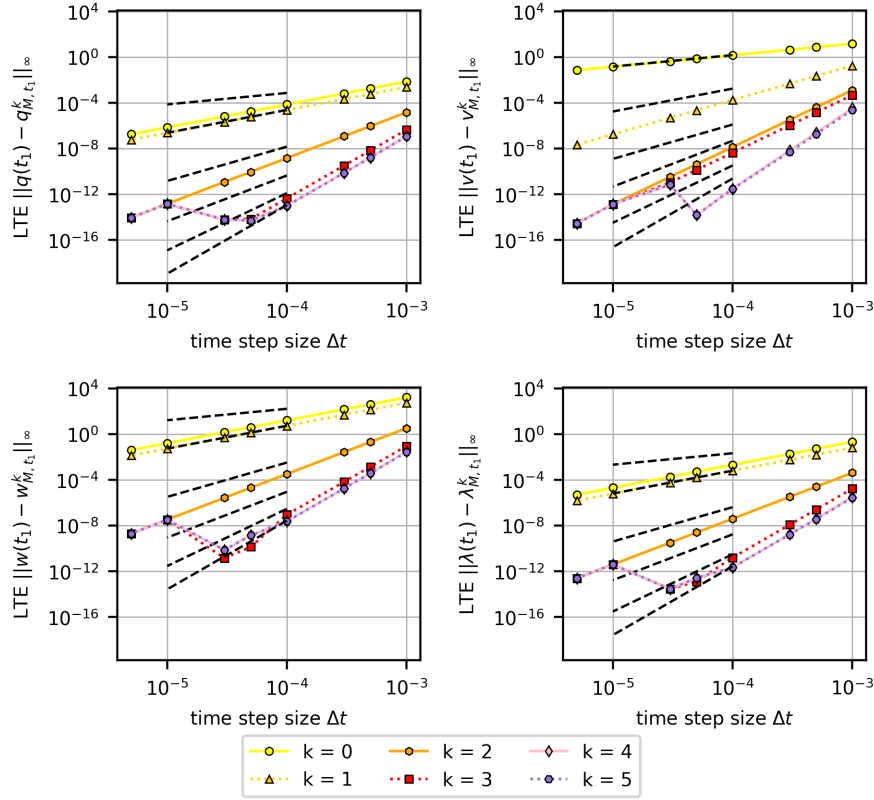


Fig. 6 Local truncation error in \mathbf{q} , \mathbf{v} , \mathbf{w} , and λ against time step sizes Δt for the constrained SDC scheme using $Q_{\Delta}^{\text{MIN-SR-NS}}$ applied to Andrews' problem for each iteration $k = 0, \dots, 2M - 1$ with $M = 3$. Black dashed lines indicate the reference order. Top row: Errors in \mathbf{q} and \mathbf{w} . Bottom row: Errors in \mathbf{w} and λ .

constraint

$$\mathbf{0} = \mathbf{g}_{\mathbf{q}\mathbf{q}}(\mathbf{q}(t))(\mathbf{v}(t), \mathbf{v}(t)) + \mathbf{G}(\mathbf{q}(t))\mathbf{w}(t) \quad (66)$$

by

$$\mathbf{0} = \mathbf{g}(\mathbf{q}(t)) \quad (67)$$

and the DAE of index one (65) is then obtained by differentiating (67) twice [12, Chap. VII.7]. The setup with the explicit functions and the matrices can be found in the reference just cited.

The implicit system at each collocation node is solved by Newton's method with tolerance $\text{tol}_{\text{newton}} = 10^{-14}$.

Figure 6 shows the order of accuracy in each iteration for the constrained SDC scheme with MIN-SR-NS preconditioning in each of the unknowns in Andrews' squeezer. In \mathbf{q} , \mathbf{w} , and λ the provisional solution is already of order two. After $k = 1$ and $k = 2$ iterations the solution is gain one order more than

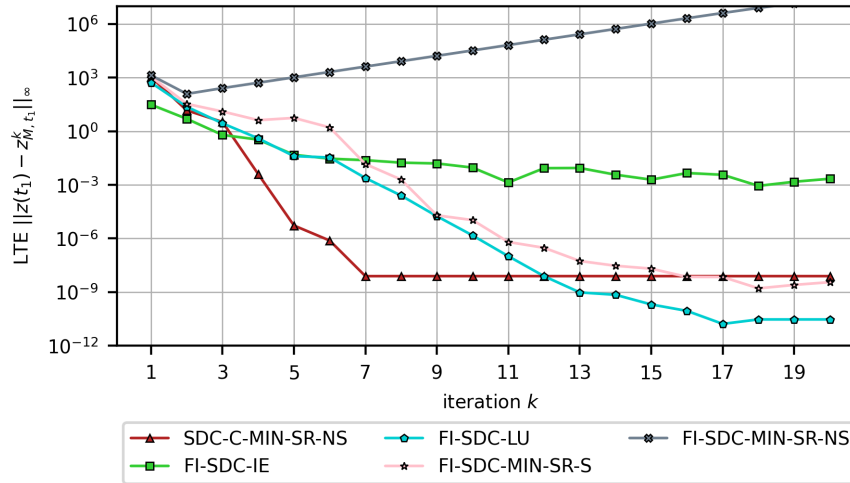


Fig. 7 Local truncation error in z versus iterations of FI-SDC schemes for one time step of size $\Delta t = 10^{-3}$ and $M = 6$ nodes. The convergence is compared with the SDC-C scheme using $Q_{\Delta}^{\text{MIN-SR-NS}}$.

expected. Thus, the final order of the SDC scheme (determined by the underlying quadrature rule) is reached after three iterations. This is different to the order behavior in \mathbf{v} : The provisional solution is of order one as expected, and after $k = 1$ and $k = 3$ iterations the numerical solution gains two orders. The final order of accuracy is achieved after four iterations the numerical solution achieves the final order of the scheme. As for the linear problem the occurrence of the phenomenon of order jumps cannot be explained, but it is a nice feature to save costs in order to achieve the desired accuracy.

In Figure 7 the global error in the algebraic variables versus the iterations for various SDC schemes in the first time step is shown. In FI-SDC, numerical integration of the algebraic variables slows down their convergence, thereby reducing the overall efficiency of the method. In particular, the Q_{Δ}^{IE} and $Q_{\Delta}^{\text{MIN-SR-S}}$ preconditioners lead to noticeably slower convergence, with the former matrix being well known for its poor convergence properties. In contrast, the FI-SDC-LU method appears to effectively mitigate this slowdown. The FI-SDC-MIN-SR-NS method diverges, which is consistent with the expectation that treating the algebraic variables in a non-stiff manner corresponds to a stiff limit, see Remark 1. The SDC schemes based on $Q_{\Delta}^{\text{Picard}}$ are not shown here, since the explicit FI-SDC-Picard method leads to a linear system with singular coefficient matrix.

Computational costs in terms of wall-clock time versus the error in \mathbf{q} at end time T for different SDC-C methods using $M = 6$ nodes are shown in Figure 8. MIN-SR-NS and MIN-SR-S precondition the constrained SDC method with similar effort where MIN-SR-NS is more efficient since it is tailored for non-stiff problems and the differential equations are non-stiff. Their numerical

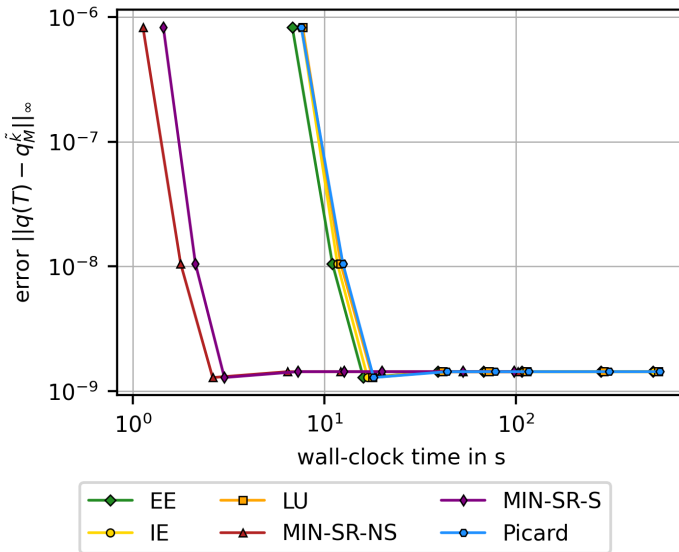


Fig. 8 Wall-clock time against absolute error in q at end time $T = 0.03$ for constrained SDC using $M = 6$ Radau IIA nodes for several choices of Q_Δ across different time step sizes Δt .

solutions are computed faster than using the other preconditioning techniques being expected to their serial nature. From all the serial methods SDC-C-EE performs best that can be expected due to the non-stiffness.

In Figure 9 SDC-C and SI-SDC with LU and MIN-SR-NS preconditioning, the Radau methods and the DOPRI5 method are opposed to each other. Again, the parallelized SDC methods SDC-C-MIN-SR-NS and SI-SDC-MIN-SR-NS show a clear advantage in computational runtime over their serial counterparts with LU preconditioning. Furthermore, between the parallel methods and the serial ones, a large gap occurs that can be explained by the fact that the LU preconditioner is tailored for stiff problems and thus works worse for non-stiff problems. Compared with the Runge-Kutta methods, the parallel schemes clearly outperform them since the Radau schemes are less efficient for larger dense systems to be solved in each time step. DOPRI5 also needs more time to compute the systems at each stage via forward substitution, and the benefit of using parallelism in schemes for larger systems becomes visible. SDC-C-MIN-SR-NS computes a numerical solution with an accuracy of $1.4 \cdot 10^{-9}$ almost ten times faster than DOPRI5, 7.8 times faster than RadauIIA5, and 3.5 times faster than RadauIIA7. The SI-SDC method with MIN-SR-NS preconditioning is quite competitive as it computes a numerical solution for the same accuracy faster by a factor of 7.9 than DOPRI5, 6.1 times faster than RadauIIA5, and 2.7 times faster than RadauIIA7.

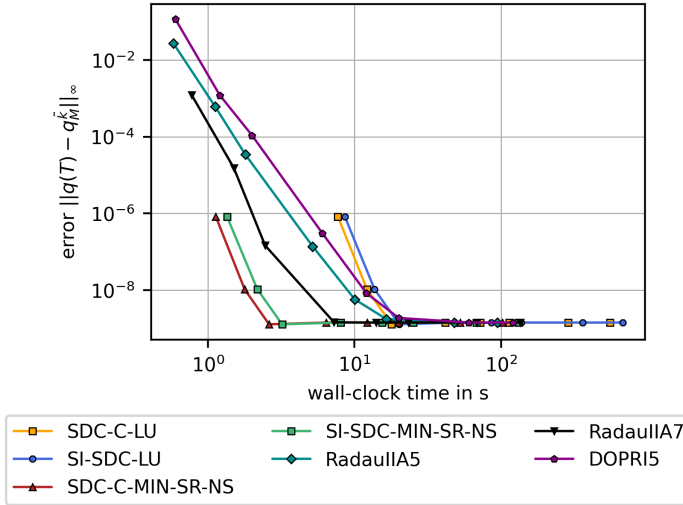


Fig. 9 Wall-clock time versus absolute error in q at end time $T = 0.03$ for different SDC variants using $M = 6$ collocation nodes for LU and MIN-SR-NS preconditioning compared with different Runge-Kutta methods for different time step sizes Δt .

4.3 Reaction-diffusion problem

We consider the stiff reaction-diffusion problem formulated as a partial DAE (PDAE)

$$\begin{aligned} \frac{\partial \mathbf{u}}{\partial t}(\mathbf{x}, t) &= \frac{\partial^2 \mathbf{u}}{\partial \mathbf{x}^2}(\mathbf{x}, t) + \mathbf{u}(\mathbf{x}, t) \frac{\partial \mathbf{w}}{\partial \mathbf{x}}(\mathbf{x}, t) + \mathbf{f}(\mathbf{x}, t), \\ \frac{\partial \mathbf{v}}{\partial t}(\mathbf{x}, t) &= \frac{\partial^2 \mathbf{v}}{\partial \mathbf{x}^2}(\mathbf{x}, t) - \mathbf{v}(\mathbf{x}, t) \frac{\partial \mathbf{w}}{\partial \mathbf{x}}(\mathbf{x}, t) + \mathbf{g}(\mathbf{x}, t), \\ \mathbf{0} &= -\mathbf{u}(\mathbf{x}, t) - \mathbf{v}(\mathbf{x}, t) - \frac{\partial^2 \mathbf{w}}{\partial \mathbf{x}^2}(\mathbf{x}, t) \end{aligned} \quad (68)$$

with differential variables $\mathbf{u}(\mathbf{x}, t), \mathbf{v}(\mathbf{x}, t) \in \mathbb{R}^n$ and algebraic variable $\mathbf{w}(\mathbf{x}, t) \in \mathbb{R}^n$ being concentrations, source terms $\mathbf{f}(\mathbf{x}, t), \mathbf{g}(\mathbf{x}, t) \in \mathbb{R}^n$ in the time interval $[0, 0.25]$, and the spatial grid $x_i = i\Delta x$, $\Delta x = \frac{1}{n}$ in $[0, 1]$ for $i = 0, \dots, n-1$ with $n = 256$ degrees of freedom. The source terms are constructed such that the exact solutions of the problem are

$$\begin{aligned} \mathbf{u}(\mathbf{x}, t) &= A \sin(2\pi \mathbf{x}) \exp(t), & \mathbf{v}(\mathbf{x}, t) &= B \sin(2\pi \mathbf{x}) \exp(t), \\ \mathbf{w}(\mathbf{x}, t) &= \frac{A+B}{4\pi^2} \sin(2\pi \mathbf{x}) \exp(t) \end{aligned}$$

with $A = B = -1$, i.e.,

$$\begin{aligned} \mathbf{f}(\mathbf{x}, t) &= \frac{\partial \mathbf{u}}{\partial t}(\mathbf{x}, t) - \frac{\partial^2 \mathbf{u}}{\partial \mathbf{x}^2}(\mathbf{x}, t) - \mathbf{u}(\mathbf{x}, t) \frac{\partial \mathbf{w}}{\partial \mathbf{x}}(\mathbf{x}, t), \\ \mathbf{g}(\mathbf{x}, t) &= \frac{\partial \mathbf{v}}{\partial t}(\mathbf{x}, t) - \frac{\partial^2 \mathbf{v}}{\partial \mathbf{x}^2}(\mathbf{x}, t) + \mathbf{v}(\mathbf{x}, t) \frac{\partial \mathbf{w}}{\partial \mathbf{x}}(\mathbf{x}, t). \end{aligned}$$

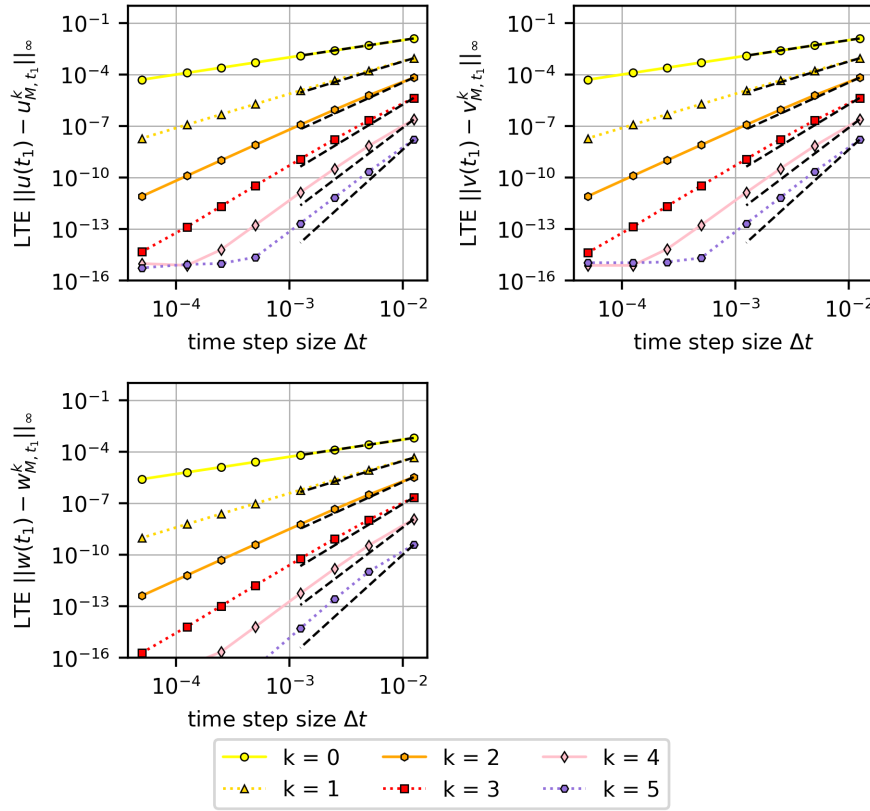


Fig. 10 Local truncation error in \mathbf{u} , \mathbf{v} and \mathbf{w} against time step sizes Δt for the constrained SDC scheme using Q_{Δ}^{TE} for the reaction-diffusion problem (68) for each iteration $k = 0, \dots, 2M - 1$ with $M = 3$. Black dashed lines indicate the reference order. Top row: Errors in \mathbf{u} and \mathbf{v} . Bottom row: Error in \mathbf{w} .

Periodic boundary conditions

$$\mathbf{u}(0, t) = \mathbf{u}(1, t), \quad \mathbf{v}(0, t) = \mathbf{v}(1, t), \quad \mathbf{w}(0, t) = \mathbf{w}(1, t)$$

are chosen. Initial conditions are obtained by evaluating the exact solutions at initial time $t_0 = 0$, i.e., $\mathbf{u}_0(\mathbf{x}) = \mathbf{u}(\mathbf{x}, 0)$, $\mathbf{v}_0(\mathbf{x}) = \mathbf{v}(\mathbf{x}, 0)$ and $\mathbf{w}_0(\mathbf{x}) = \mathbf{w}(\mathbf{x}, 0)$. For a comprehensive analysis to local and global solutions the reader is referred to [3]. The computations were performed in the spectral space using the discrete Fourier transformation and afterwards shifted back to the real space, ensuring high spatial accuracy of the numerical solutions. Newton's method is used to solve the implicit system in spectral space at each node. The tolerance is coupled to the time step size by

$$tol_{\text{newton}} = \frac{tol_{\text{ref}} \Delta t}{\Delta t_{\text{ref}}}$$

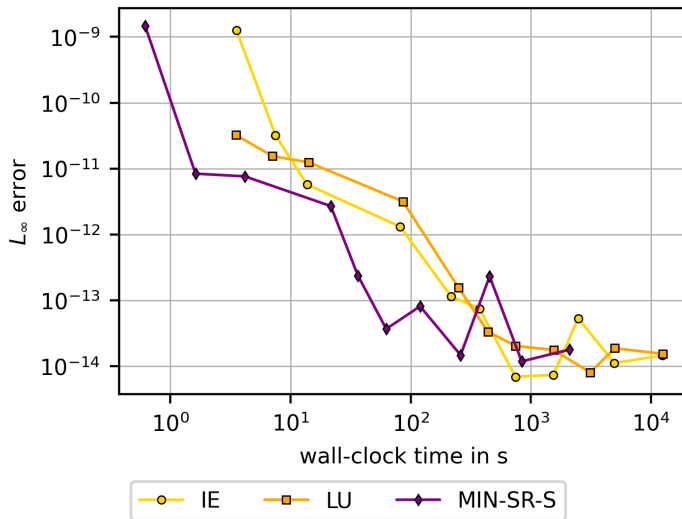


Fig. 11 Wall-clock time against L_∞ error for constrained SDC using $M = 6$ Radau IIA nodes for several choices of \mathbf{Q}_Δ across different time step sizes Δt .

with $tol_{ref} = 1.3 \cdot 10^{-12}$ and $\Delta t_{ref} = 2.6 \cdot 10^{-3}$ to balance accuracy and efficiency. For $\Delta t > \Delta t_{ref}$, a relaxed tolerance reduces the computational cost of the nonlinear solves, while for $\Delta t < \Delta t_{ref}$ a stricter tolerance is imposed to match the higher temporal accuracy. In the latter case, the Newton iteration typically terminates after the maximum number of iterations without reaching the prescribed tolerance, but still benefits the overall solution accuracy. This strategy provides an effective compromise between runtime and accuracy.

In Figure 10 the order of accuracy for \mathbf{u} , \mathbf{v} , and \mathbf{w} in each iteration for SDC-C-IE is shown. After $k = 3$ iterations, the expected orders are barely achieved. Although the IE preconditioner is suitable for stiff problems, it is also known for its slow convergence, but this is observed for LU and MIN-SR-S preconditioning as well. In our numerical experiments (not shown here), the observed order in \mathbf{w} for SI-SDC at iteration k does not fully match the prediction of Theorem 3, and in general this is also not true for FI-SDC. Especially, numerical integration inside the algebraic constraints does lead to slower convergence of the algebraic constraints implying that the convergence rate is reduced at least in \mathbf{w} , see Remark 2. A comprehensive theoretical analysis could provide further insight into this observation, but is left for future work.

Figure 11 shows the costs of the constrained SDC scheme using the stiff choices of \mathbf{Q}_Δ matrices. The constrained SDC scheme benefits from the parallel MIN-SR-S preconditioning by saving computational time. It computes the solution quite faster than the serial schemes SDC-C-IE and SDC-C-LU. While SDC-C-IE and SDC-C-LU show similar runtimes, SDC-C-IE yields a higher overall accuracy for moderate time step sizes. The non-stiff choices \mathbf{Q}_Δ^{EE} , $\mathbf{Q}_\Delta^{Picard}$, and $\mathbf{Q}_\Delta^{MIN-SR-NS}$ result in diverging methods due to the stiffness nature of the

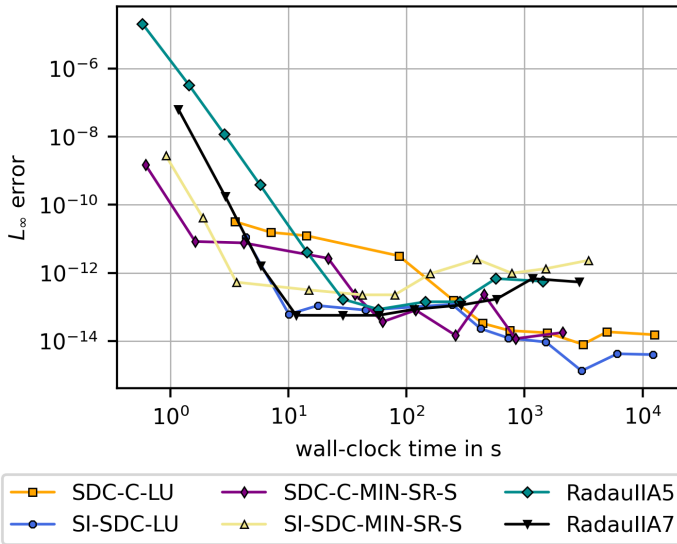


Fig. 12 Wall-clock time versus L_∞ error for different SDC variants using $M = 6$ collocation nodes for LU and MIN-SR-S preconditioning compared with Radau IIA methods of order 5 and 7 for different time step sizes Δt .

problem, where the latter one yields an implicit scheme. Thus, they are not recommended for this problem.

In Figure 12 the costs versus the accuracy of different SDC variants and the Radau methods are opposed to each other. For larger Δt the schemes SDC-C-MIN-SR-S and SI-SDC-MIN-SR-S benefit from the coupled Newton tolerance to the time step size and outperform the Radau IIA method of order 7 in runtime and accuracy. While the fifth-order Radau IIA method computes as fast as SDC-C-MIN-SR-S and faster than SI-SDC-MIN-SR-S, both SDC variants are still provide better accuracy. The serial SDC variants using the LU-trick are less favourable here due to their high computational costs. The SI-SDC-LU scheme as much more accurate than the SDC-C-LU although they have similar runtimes. The accuracy can be improved by adjusting the convergence parameters but also yields higher computational costs.

For different SDC-C and SI-SDC schemes the absolute value of the algebraic constraints across iterations is shown in Figure 13. Although the SI-SDC scheme is suitable for semi-explicit DAEs it cannot be expected that the algebraic equations are approximately zero along the iteration process, see Remark 2. It is obvious that the value of g is still converging towards zero whereas the value of g in the SDC-C scheme during the iterations is almost zero every-time thanks to the construction of the scheme.

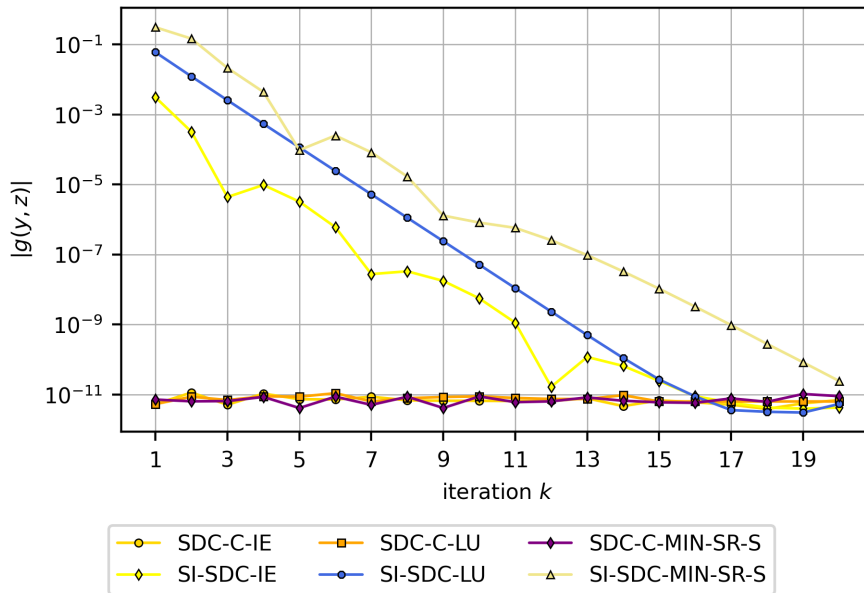


Fig. 13 Absolute value of algebraic equations versus iterations of different **SDC-C** and **SI-SDC** schemes for one time step of size $\Delta t = 0.125$ and $M = 6$ nodes.

5 Conclusion

The solution of DAEs requires a tailored solver to efficiently compute a numerical solution with high accuracy. The SDC method is a high-order scheme that iteratively computes a solution by correcting the provisional approximation after each iteration. Under certain assumptions, the numerical solution gains one order per iteration [24]. In [14], a SDC method for general IDEs and a semi-integrating variant for semi-explicit DAEs is proposed. The traditional idea of SDC is carried over to the semi-explicit DAE case to derive the **SDC-C** scheme. It only integrates the differential equations with spectral quadrature and retains the algebraic constraints as an implicit condition in the system. The efficiency of the scheme is studied using various choices of \mathbf{Q}_Δ matrices. Especially, we study the scheme for diagonal \mathbf{Q}_Δ that allows the scheme to be parallelized across the method.

We have shown that each iteration of the **SDC-C** scheme improves the numerical solution in differential and algebraic variables of index-one problems by one where the idea of the proof of the result from [24] is carried over. This is confirmed in numerical experiments where we considered three test scenarios: The linear test DAE, the nonlinear problem describing Andrews' squeezing mechanism, and the reaction-diffusion problem as a PDAE. In work versus precision plots, the efficiency of the different schemes is evaluated where the work is measured in terms of runtime. The proposed scheme is compared with other

SDC methods and existent DAE methods that includes half-explicit Runge–Kutta schemes and Radau IIA solvers. We have shown that the **SDC–C** scheme is competitive with all the different schemes. The proposed **SDC–C** method consistently achieves a significantly higher accuracy than the Radau IIA solvers for identical time step sizes. In addition, for several test cases, **SDC–C** attains this improved accuracy at a comparable or even reduced computational cost, resulting in shorter runtimes than the Radau IIA methods. This highlights the potential of **SDC–C** as an efficient and accurate alternative to classical implicit Runge–Kutta solvers. Moreover, for the test problems considered, the presented scheme also proves to be more efficient than the other SDC variants, highlighting its favorable accuracy–efficiency balance.

Data Availability

The data supporting the findings of this study are generated by numerical simulations. The code used to reproduce all results is publicly available at https://github.com/lisawim/pySDC/tree/sdc_dae_analysis_paper.

Funding

This work was partially supported through the PLEIADES computing cluster, which is funded by the Deutsche Forschungsgemeinschaft (DFG, grant No. INST 218/78-1 FUGG) and the Bundesministerium für Bildung und Forschung (BMBFTR).

Declarations

Conflict of Interest

The author declares that there is no conflict of interest.

Competing Interests

The author declares no competing interests.

Ethics Approval

Not applicable.

Consent to Participate

Not applicable.

Consent for Publication

Not applicable.

References

1. Andrews, G.C., Ormrod, M.K.: Advent: A Simulation Program for Constrained Planar Kinematic and Dynamic Systems. In: Proceedings of the ASME Design Engineering Technical Conference (DETC), 86-DET-97. American Society of Mechanical Engineers (ASME), Department of Mechanical Engineering, University of Waterloo, Columbus, Ohio (1986)
2. Ascher, U.M., Petzold, L.R.: Computer Methods for Ordinary Differential Equations and Differential-Algebraic Equations. SIAM, Philadelphia, PA (1998). doi:10.1137/1.9781611971392
3. Benabdallah, S.A., Souilah, M.: Existence and Uniqueness of Local and Global Solutions for a Partial Differential-Algebraic Equation of Index one. Preprint, arXiv:2411.15658 [math.AP] (2025). doi:10.48550/arXiv.2411.15658
4. Bergische Universität Wuppertal: Pleiades high-performance computing cluster (2025). URL <https://pleiades.uni-wuppertal.de>. Accessed: 2025-08-22
5. Brenan, K.E., Campbell, S.L., Petzold, L.R.: Numerical Solution of Initial-Value Problems in Differential-Algebraic Equations, *Classics in Applied Mathematics*, vol. 14, unabridged, corr. republ. edn. SIAM, Philadelphia, PA (1996). doi:10.1137/1.9781611971224
6. Bu, S., Huang, J., Minion, M.L.: Semi-implicit Krylov deferred correction methods for differential algebraic equations. *Math. Comput.* **81**(280), 2127–2157 (2012). doi:10.1090/S0025-5718-2012-02564-6
7. Čaklović, G., Lunet, T., Götschel, S., Ruprecht, D.: Improving efficiency of parallel across the method spectral deferred corrections. *SIAM J. Sci. Comput.* **47**(1), A430–A453 (2025). doi:10.1137/24M1649800
8. Dormand, J.R., Prince, P.J.: A family of embedded Runge-Kutta formulae. *J. Comput. Appl. Math.* **6**, 19–26 (1980). doi:10.1016/0771-050X(80)90013-3
9. Dutt, A., Greengard, L., Rokhlin, V.: Spectral deferred correction methods for ordinary differential equations. *BIT* **40**(2), 241–266 (2000). doi:10.1023/A:1022338906936
10. Emmett, M., Minion, M.L.: Toward an efficient parallel in time method for partial differential equations. *Commun. Appl. Math. Comput. Sci.* **7**(1), 105–132 (2012). doi:10.2140/camcos.2012.7.105
11. Hairer, E., Lubich, C., Roche, M.: The Numerical Solution of Differential-Algebraic Systems by Runge-Kutta Methods, *Lect. Notes Math.*, vol. 1409. Springer, Cham (1989). doi:10.1007/BFb0093947
12. Hairer, E., Wanner, G.: Solving Ordinary Differential Equations. II: Stiff and Differential-Algebraic Problems, *Springer Series in Computational Mathematics*, vol. 14, reprint of the 1996 2nd revised ed. edn. Springer, Berlin (2010). doi:10.1007/978-3-642-05221-7
13. Huang, J., Jia, J., Minion, M.: Accelerating the convergence of spectral deferred correction methods. *J. Comput. Phys.* **214**(2), 633–656 (2006). doi:10.1016/j.jcp.2005.10.004
14. Huang, J., Jia, J., Minion, M.: Arbitrary order Krylov deferred correction methods for differential algebraic equations. *J. Comput. Phys.* **221**(2), 739–760 (2007). doi:10.1016/j.jcp.2006.06.040
15. Kremling, G., Speck, R.: Convergence of multilevel spectral deferred corrections. *Commun. Appl. Math. Comput. Sci.* **16**(2), 227–265 (2021). doi:10.2140/camcos.2021.16.227
16. Minion, M.L.: Semi-implicit spectral deferred correction methods for ordinary differential equations. *Commun. Math. Sci.* **1**(3), 471–500 (2003). doi:10.4310/CMS.2003.v1.n3.a6
17. Pfister, E., Stiller, J.: Robust semi-implicit multilevel SDC methods for conservation laws. Preprint, arXiv:2504.18526 [math.NA] (2025). URL <https://arxiv.org/abs/2504.18526>

18. Qu, W., Brandon, N., Chen, D., Huang, J., Kress, T.: A numerical framework for integrating deferred correction methods to solve high order collocation formulations of ODEs. *J. Sci. Comput.* **68**(2), 484–520 (2016). doi:10.1007/s10915-015-0146-9
19. Ruprecht, D., Speck, R.: Spectral deferred corrections with fast-wave slow-wave splitting. *SIAM J. Sci. Comput.* **38**(4), a2535–a2557 (2016). doi:10.1137/16M1060078
20. Saupe, T., Götschel, S., Lunet, T., Ruprecht, D., Speck, R.: Adaptive time step selection for spectral deferred correction. *Numer. Algorithms* **100**(1), 369–393 (2025). doi:10.1007/s11075-024-01964-z
21. Speck, R.: Parallelizing spectral deferred corrections across the method. *Comput. Vis. Sci.* **19**(3–4), 75–83 (2018). doi:10.1007/s00791-018-0298-x
22. Speck, R., Lunet, T., Baumann, T., Wimmer, L., Akramov, I., Rosilho de Souza, G., Fritz, J., Shipton, J.: Parallel-in-time/pysdc (2025). doi:10.5281/zenodo.15196003. URL <https://doi.org/10.5281/zenodo.15196003>. Software release on Zenodo
23. Weiser, M.: Faster SDC convergence on non-equidistant grids by DIRK sweeps. *BIT* **55**(4), 1219–1241 (2015). doi:10.1007/s10543-014-0540-y
24. Xia, Y., Xu, Y., Shu, C.W.: Efficient time discretization for local discontinuous Galerkin methods. *Discrete Contin. Dyn. Syst., Ser. B* **8**(3), 677–693 (2007). doi:10.3934/dcdsb.2007.8.677